SOLAR DRIVEN HYDROGEN FUEL ELECTRO-GENERATION FROM WATER

Thesis submitted towards the partial fulfilment of Master of Engineering degree in Chemical Engineering

by

SUDIPTA GHOSH

Examination Roll no: M4CHE24018

Class Roll No.: 001810302018

Registration No.: 163446

Session: 2022 – 2024

Under the guidance of

Dr. Raj Kumar Das

DEPARTMENT OF CHEMICAL ENGINEERING

JADAVPUR UNIVERSITY

Kolkata - 700032

CERTIFICATION

This is to certify that **Mr. Sudipta ghosh**, final year student in Master of Chemical Engineering examination in the department of Chemical Engineering, Jadavpur University, bearing Registration No: 163446 has successfully completed the thesis work entitled **"SOLAR DRIVEN HYDROGEN FUEL ELECTRO-GENERATION FROM WATER"** under the guidance of **Dr. Raj Kumar Das** during his master degree curriculum. This work has not been reported earlier anywhere and can be approved for submission in partial fulfilment of the requirements for the Master of Engineering in Chemical Engineering.

30/05/24

Dr. Raj Kumar Das

Project Supervisor

Chemical Engineering Department

Jadavpur University

Assistant Professor
CHEMICAL ENGINEERING DEPARTMENT
JADAVPUR UNIVERSITY
Kolkata-700 032

Assistant Professor
CHEMICAL ENGINEERING DEPARTMENT
JADAVPUR UNIVERSITY
Kolkata-700 032

30/5/24

Head of the Department
Chemical Engineering Department
Jadavpur University

HEAD
CHEMICAL ENGINEERING DEPARTMENT
JADAVPUR UNIVERSITY
Kolkata-700 032

Dipak Laha 30/5/24

Dean
Faculty of Engineering & Technology
Jadavpur University

DEAN
Faculty of Engineering & Technology
JADAVPUR UNIVERSITY
KOLKATA-700 032

DECLARATION OF ORIGINALITY AND COMPLIANCE OF ACADEMIC ETHICS

I hereby declare that this thesis contains literature survey and original research work by the undersigned candidate, as part of his "***Master of Engineering in Chemical Engineering***" studies. All information in this document have been obtained and presented in accordance with academic rules and ethical conduct.

I also declare that, as required by these rules and conduct, I have fully cited and referenced all material and results that are not original to research work.

Name: **SUDIPTA GHOSH**

Registration No.: 163446

Thesis Title: **SOLAR DRIVEN HYDROGEN FUEL ELECTRO-GENERATION FROM WATER.**

Signature: Sudipta Ghosh

Date: 30.05.24

CERTIFICATE OF APPROVAL

This thesis is hereby approved as creditable study of an engineering subject carried out and presented in a manner satisfactory to warrant its acceptance as prerequisite to the degree for which it has been submitted. It is understood by this approval that undersigned don't endorse or approve any statement made, opinion expressed or conclusion drawn therein but approve the thesis only for purpose of which it is submitted.

Sudipta Ghosh 30.05.24

.....

Sudipta ghosh

Department of Chemical Engineering

Jadavpur University

ACKNOWLEDGEMENT

Though the following project is individual project work, but I would have never been successful in completing my work in a smooth manner without help, guidance, assistance, and inspiration from a lot of people. At the start of this report, I would like to thank all those persons who have helped me in this endeavor. Without their guidance and help it would not be possible for me to progress and plan about this project.

I would sincerely express my gratitude towards my project guides Dr. Raj kumar Das for their valuable guidance and cooperation and for providing me the opportunity to accomplish the project. Without their guidance and assistance, I would never be able to work successfully in this area. I am greatly thankful to them for guiding me always throughout my project work.

I would like to thank all my lab mates who consistently helped me while performing and planning this project.

I would also like to express gratitude to HOD and all faculties of the Chemical Engineering Department, Jadavpur University.

Thanking you,
Sudipta ghosh
Class Roll Number – 001810302018
Registration Number – 163446 of 2022-24
M.E. 2nd Year
EXAMINATION ROLL.NO- M4CHE24018

Abstract

Hydrogen energy, as clean and efficient energy, is considered significant support for the construction of a sustainable society in the face of global climate change and the looming energy revolution. Hydrogen is one of the most important chemical substances on earth and can be obtained through various techniques using renewable and nonrenewable energy sources. However, the necessity for a gradual transition to renewable energy sources significantly hampers efforts to identify and implement green hydrogen production paths. Therefore, this paper's objective is to provide a technological review of the systems of hydrogen production from solar energy utilizing several types of water electrolyzers. The current paper starts with a short brief about the different production techniques. A detailed comparison between water electrolyzer types and a complete illustration of hydrogen production techniques using solar and wind are presented with examples, after which an economic assessment of green hydrogen production by comparing the costs of the discussed renewable sources with other production methods. One of the main challenges hindering the development of efficient photocathodes is the limited efficiency of the photocathodes themselves, resulting in relatively low current densities being produced. In this context, we bring to light a novel approach that embodies a fresh design principle aimed at enhancing the effectiveness of photocathodes significantly. This innovative approach hinges on the concept of outer-sphere reduction. An intriguing outcome of this methodology is observed when dioxygen is directly reduced from dye-sensitized nickel oxide (NiO), leading to the generation of hydrogen peroxide (H2O2). The experimental results demonstrate that under conditions involving oxygen and visible light, NiO photocathodes sensitized approaching the thermodynamic potential for generation of O2/H2O2 in nearly neutral water. This achievement marks a significant milestone, positioning these particular NiO photocathodes as one of the most efficient reported thus far for multiproton /multielectron transformations. The photoelectrosynthesis mechanism is initiated with the generation of superoxide, which subsequently undergoes disproportionation to yield H2O2. The effectiveness of this disproportionation-driven charge separation strategy lies in its ability to circumvent the inherent difficulties associated with separating electron−hole pairs in photo cathodes connected to inner sphere electrocatalysts. Embracing this innovative approach not only addresses existing challenges but also paves the way for novel applications in photoelectron synthesis cells. Finally, the challenges that face the mentioned production methods are illuminated in the current review.

Contents

1. Introduction
2. Literature review
   2.1. chemical compound from plant extract
3. Experimental chemicals material and method
   3.1. Chemicals and reagents
   3.2. Preparation of bio-extract
   3.3. NiO NPs synthesis methodology
   3.4. Electrochemical studies
      3.4.1. Fabrication NiO NPs embedment support on graphite
      3.4.2. Electroanalytic methods
4. Solar driven hydrogen production
   4.1. Hydrogen production technologies
5. Water electrolyzer
   5.1. Principle of water electrolysis
   5.2. Thermodynamic
   5.3. Faradays law
6. Types of electrolyzer
   6.1. Proton exchange membrane electrolyzer
   6.2. Alkaline water electrolyzer
   6.3. Alkaline anion exchange membrane electrolyzer
   6.4. High temperature steam electrolyzer
   6.5. Solid oxide electrolyzer
7. Challenges of water electrolysis
8. Cell voltage (difference of potential)
9. Green electricity production system
10. PV/H_2 case studies
11. PV/H_2 system
12. Economic assessment of green hydrogen production
13. Economic challenges
14. Ways of storing renewal hydrogen
   14.1. Geological hydrogen storage
   14.2. Liquidfied hydrogen storage
   14.3. Compressed hydrogen storage
   14.4. Material based storage
15. Future prospects
16. conclusion

What is green hydrogen fuel ?

Hydrogen, a versatile and promising fuel with great potential, has been recognized for its positive impact on the environment due to its clean and renewable nature. Its production from a variety of domestic resources, such as natural gas, nuclear power, biomass, and renewable sources like solar power, makes it an attractive option for fueling both transportation and electricity generation applications. One of the key benefits of using hydrogen as a fuel is that it only generates water as a byproduct when consumed in a fuel cell, making it incredibly environmentally friendly. Moreover, the versatility of hydrogen extends beyond its eco-friendly properties and reaches various sectors, including automotive, residential, and portable power solutions. Its ability to serve as an energy carrier plays a critical role in storing, moving, and delivering energy generated from different sources, contributing to a more sustainable and efficient energy system.

Currently, the two most common methods for producing hydrogen are natural gas reforming, a thermal process, and electrolysis, which includes solar-driven processes. Ongoing research in this field is dedicated to further enhancing the efficiency, reducing production costs, and increasing the overall sustainability of hydrogen production techniques. These advancements are crucial in ensuring that hydrogen remains a viable and eco-conscious fuel option for the future.

1. Introduction

India weather is currently hotter than it has been in previous years due to global warming, which is caused by various forms of pollution brought on by the burning of fossil fuels. using fossil fuels. Fuels release a variety of pollutants into the atmosphere, including sulfur dioxide, nitrogen oxides, particulate matter, ground-level ozone, carbon monoxide, carbon dioxide, and volatile organic compounds like benzene and some heavy metals. These byproducts of burning fossil fuels act as an insulating barrier to prevent heat from leaving the Earth's surface. Future years are expected to see an increase in temperature, based on the annual temperature anomaly simulated by the Providing Regional Climates for Impacts Studies. The findings of this anomaly are summarized in. Thus, the development of green and renewable energy is necessary.

- the use of fossil fuels is responsible for climate change.
- deposits of fossil fuels are limited.
- the price of the fossil fuels is increasing.

- there is a need for a fuel that is environmentally safe.

The primary cause of climate change is CO2 emission resulting from the burning of fossil fuels such as coal, oil, and natural gas. These emissions are anticipated to have severe consequences for Earth. Consequently, urgent measures are required to reduce CO2 emissions and explore sustainable alternatives to fossil fuels, especially in light of aggressive international climate policies aimed at phasing out coal use. Among the promising alternatives is hydrogen (H2), a versatile energy carrier garnering unprecedented global attention due to its high gravimetric energy density of approximately 120 MJ kg−1, minimal greenhouse gas emissions, and compatibility with existing industrial infrastructure and fossil fuel-powered plants. The growing global population's reliance on fossil fuels has caused significant environmental issues, prompting the need for a cost-effective, reliable, and eco-friendly primary energy source with minimal carbon emissions. As such, it is imperative to find and implement a renewable and universally accessible clean energy source. A prime example of this shift is the installation of renewable energy plants in arid regions, necessitating efficient storage systems to counter intermittency. Hydrogen emerges as a viable candidate for the transition to clean energy due to its ability to be stored, transported, and combusted with high calorific value, making it a feasible replacement for traditional fuels. The eco-friendly production process of hydrogen stands out as a key attribute for environmental enhancement and sustainable development. Moreover, hydrogen's application in fuel cells offers a clean energy solution for electricity generation, boasting high efficiency and zero toxic emissions. This paper aims to offer a comprehensive overview of hydrogen production techniques, particularly focusing on water electrolysis powered by solar energy. It includes a detailed examination of various electrolyzer types, highlighting their respective advantages and disadvantages. The economic feasibility of these production systems is also analyzed to outline the costs and challenges associated with each technique. By exploring these topics, this paper aims to support researchers in gaining a deeper comprehension of clean hydrogen production methods via solar-powered water electrolysis.

One of the common applications of hydrogen peroxide (H2O2) is its vital role as a precursor in the generation of hydroxyl radicals (OH, as represented in Equation (1)) within advanced oxidation processes (AOPs) utilized for the efficient treatment of wastewater, as highlighted in various studies [1,2]. Additionally, a noteworthy outcome of the decomposition reaction of

H_2O_2 is the production of water and oxygen, emphasizing its environmentally friendly nature. Thus, hydrogen peroxide stands out as a highly significant and sustainable reagent with widespread applications across various industries, especially in the realm of wastewater treatment, due to its versatile and eco-friendly properties.

$Fe^{2+} + H_2O_2 \rightarrow Fe^{3+} + OH + OH^-$ ($E^\circ = 2.5106$ V vs. Ag/AgCl) (1)

In an electro-Fenton process (EFP), H_2O_2 (Eq. (2)) and Fe^{2+} (Eq. (3)) are electrochemically generated in-situ, separately or simultaneously [1,3].

$2H^+ + O_2 + 2e \longrightarrow H_2O_2$ ($E^\circ = 0.393$ V vs. Ag/AgCl) (2)

$Fe^{3+} + e^- \rightarrow Fe^{2+}$ ($E^\circ = 0.482$ V vs. Ag/AgCl) (3)

Expanding on the discussion of the electro-generation of hydrogen peroxide in an acidic solution through the reduction of dissolved oxygen at a low cathodic potential reveals a process with multifaceted benefits. Not only does this method present the advantage of cost reduction and lower hazard levels in transportation and handling compared to the use of concentrated H_2O_2, but it also signifies a promising advancement in sustainable chemistry. Furthermore, the conversion of O_2 to H_2O holds significant implications in the realms of fuel cell technology and the development of efficient metal-air batteries, showcasing its transformative potential in various practical applications. Overall, the exploration of this innovative research area illuminates a path towards greener and more efficient chemical processes with extensive real-world implications awaiting further exploration and development. [4,5].

Graphite [5,11] and carbon [1,12] based materials, such as activated carbon fiber, carbon/graphite felt, carbon nanotube, carbon sponge, and reticulated vitreous carbon, are commonly employed as cathodes in the generation of H_2O_2. These carbonaceous materials offer numerous advantages, including minimal toxicity, excellent stability, high conductivity, and low catalytic activity for H_2O_2 decomposition [12,13]. However, conventional carbonaceous materials for H_2O_2 production are plagued by challenges such as high overpotential and sluggish electron transfer kinetics [14], prompting the exploration of alternative approaches. Recent trends in research have shifted towards the utilization of nano-structured materials as electrocatalysts to address these limitations in H_2O_2 synthesis [1,15]. In particular, there is a growing emphasis on metal nanoparticles (NPs) and metal oxides NPs to boost the current efficiency of H_2O_2 formation. Notably, these advanced catalysts can be

easily immobilized on the surface of minute electrodes, offering promising avenues for enhancing the efficiency and performance of H2O2 production processes [12,16].

its ability to generate hydroxyl radicals and its environmentally friendly decomposition into water and oxygen, hydrogen peroxide is considered a relatively safe and eco-friendly reagent for wastewater treatment in AOPs. the common use of graphite and various carbon-based materials as cathodes for the generation of hydrogen peroxide (H2O2). These materials include activated carbon fiber, carbon/graphite felt, carbon nanotubes, carbon sponge, and reticulated vitreous carbon. These materials are preferred due to their low toxicity, stability, high conductivity, and low catalytic activity for H2O2 decomposition. carbonaceous materials face challenges such as high overpotential and slow kinetics of electron transfer during H2O2 generation. To address these limitations, researchers are turning to nanostructured materials as electrocatalysts for H2O2 synthesis. These nanostructured materials, such as metal nanoparticles (NPs) and metal oxides NPs, offer improved efficiency and kinetics for H2O2 formation. Graphite and carbon-based materials are commonly used as cathodes for H2O2 generation due to their favorable properties such as stability and conductivity. Traditional carbonaceous materials suffer from high overpotential and slow kinetics during H2O2 synthesis. Nanostructured materials are including metal nanoparticles (NPs) and metal oxides NPs, are being developed as electrocatalysts to enhance the efficiency and kinetics of H2O2 formation. This materials offer improved performance and can be easily immobilized on small electrodes, making them attractive for H2O2 synthesis applications. Main focus of current research is on developing advanced nanostructured materials to overcome the limitations of traditional carbonaceous materials and enhance the efficiency of hydrogen peroxide formation. Transition metal oxides nanoparticles (NPs), including NiO, Co3O4, Cu2O, MnO2, and Fe2O3, are noted for their potential to enhance electrocatalytic activity and promote electron-transfer reactions, particularly in the context of improved hydrogen peroxide (H2O2) generation. Among these, NiO holds significant versatility across various applications such as gas sensors, electrochromic devices, catalysis, fuel cell electrodes, magnetic materials, photovoltaic devices, and batteries. This versatility stems from NiO's easily interchangeable oxidation states (NiO, NiOOH , Ni (OH)2, etc. allowing for diverse functionalities. The strong interfacial interaction between NiO and carbon-based materials (electrode base or catalyst support) is highlighted as beneficial for facilitating charge transfer between these materials, further enhancing their catalytic performance. Factors such as the morphology, crystallography, and size of NiO NPs play

crucial roles in determining their catalytic activities, as indicated by numerous studies. Various synthesis techniques are employed to produce nanostructured NiO materials.[1]

- Sol-gel method
- Solvo-/hydrothermal method
- Thermal decomposition method
- Chemical spray pyrolysis
- Microemulsion method
- Microwave irradiation

These techniques enable the controlled fabrication of NiO nanoparticles with desired properties, contributing to their effectiveness as electrocatalysts for H2O2 generation and other applications mentioned above. recently, these authors have reported that the use of reducing agents (10-30 times of NPs precursors) such as sodium borohydride, hydrazine, ethylene glycol, polyvinylpyrrolidone, and sodium citrate etc. can be avoided for the synthesis of spinel Co3O4 NPs by the use of (green) analytes present in plant organs. The common plant based analytes are ascorbic acid, amino acids, and polyphenolic compounds and, they also could minimize the NPs agglomeration. But, the abundance of these analytes is affected by the cultivation condition and local climate. As squash and vegetable pear, belongs to the gourd family of Cucurbitaceae and, it is a rich source of Ascorbic Acid (0.3 mg per g dry fruit). In this work, the analytes along with present in following paper are extracted in water and employed for the synthesis of NiO NPs instead of using the chemical reductants and, perhaps, it is the first study of this kind for the NiO NPs synthesis following a green pathway. Capping agents present in the bio-extract also prevent the aggregation of NiO NPs, leading to its size and morphological control.

The mechanism of NiO NPs formation was proposed and validated by identifying the analytes using liquid chromatography-mass spectrometry (LCMS). The control experiment was conducted for the formation of NiO NPs, if any, without the use of analytes. The characterizations of NiO NPs were performed through XRD (X-ray diffraction), TGA (Thermogravimetric analysis), FTIR (Fourier-transform infrared), UV-Vis, and Raman spectroscopies, VSM (Vibrating sample magnetometry), BET (Brunauer-Emmett-Teller) isotherm, SEM (Scanning electron microscopy), and HRTEM (High-resolution transmission electron microscopy). The support/base electrode of NiO NPs was made of high-purity graphite which was fabricated by the conventional carbon paste method and, the NPs were

embedded on the support electrode with the help of Nafion as a binder material. These tests are conducted to characterize the electrochemical behavior of the graphite/NiO NPs cathode in the context of H2O2 generation. The tests likely involve varying potential sweeps to study the redox reactions involved in the process. The results from the graphite/NiO NPs cathode are compared with those obtained from bare-support (without NiO NPs) and control electrodes (possibly a standard electrode) to assess the catalytic effect of NiO NPs on H2O2 generation. The investigation into the effect of proton concentration on the yield and current efficiency of H2O2 generation suggests a study of how acidity (pH) influences the reaction kinetics and product formation. The area of the working electrode (WE), which is the graphite/NiO NPs cathode, is varied between 3.3 and 5.9 cm2. This variation allows for the determination of parameters such as limiting current density and the coefficient of DO mass transfer, providing insights into the efficiency and kinetics of the H2O2 generation reaction. [1,4]

2. Literature Review

2.1 Chemical compounds from plant extract

Gallic acid (3,4,5-Trihydroxibenzoic Acid) - Tea Leaves, Orange, Graps
Vanillic Acid - Tea, Coffee
Saponins - Garlic, Onion, Oats, Tomatoes, Spinach
Poly Saccharides – Tea
Anthocyanin - Eggplant peel, Cheery, Sweet Potatoes, Pomegranate, Strawberries
ProtoCatechuic Acid- Dried flower of hibiscus, Carrots
Chlorogenic acid - Apple, Carrot, Coffee Beans, Graps, Potatoes, Tea Leaves
Luteolin - Celery, Parsley, Brocooli, Onion Leaves, Carrot, Peppers, Cabbages, Apple skin
Tanins - Black Berries, Pomegranates
Ferulic Acid - Rice, wheat, Pineapple, Bananas, Spinach, Beetroot, Coffee Beans, Peanut
Salicylic Acid - Tomatoes, Apple, Avocado, Cherries, Graps
Caffeic Acid - Coffee, Potatoes, Sunflower Seeds.

Table – 1

SL. NO	SOURCE	TYPES OF PLANT	EXPERIMENTAL CONDITION	PARTICLE SIZE
1	H.G Gebretinsac, M.G tsegay, Z.Y nuru, et.al2021	Cactus (opuntia gicus indica)	Using nickle nitriate hexahydrate (Ni(No3)2),6H2O, Deionized water(H2O) and cactus plant The x-ray diffraction pattern of nio powder obtained from the decomposition of the precursor annealated 500 dergee c.	Avg 16nm
2	Muhammad Imran din, amnaghulan nabi, anecla rani ayesha aihetasham maria mukhtar. Et.al2018	Calotropis gigantea	80˚c temp, 90 min incubation time PH12 ,1mMh recursor concentration and 20% extract concentration.(NiNo3)2,6H2O, sodium hydroxide (naoh). 90% (v/v)methanol(ch3oh), sodium borohydride(NaBHa) distilled water(H2o)	20-40nm
3	Chitra Jeyaraj pandian, Ramesh thangam palanivel Et.al2015	Ocimum sanctum	Nickle nitrate, barium sulphate and potassium nitrate	12-36nm
4	Tanveer ali Muhammad faroon warsi , Sonia zulfigar Abdul sami,et.al2021	Seeds of lactuca serriola	Nicl2, 6H2O , crystal violetdye lactuca serriola was dissolve in ethanol and freashly synlhesized Nio nanoparticle at 20µg/ml and 10µg/ml concentration and aspectically mounted on sensitivity plates with suitable controls. Ciprofloxacin was used as positive control the sample dry into laminar flow chamber. The petri dishes were incubated at a temp entire of 37˚c per 24h.	<100nm
5	Ali haider, Muhammad ,ijaz, sidra ali,et.al2020	Ginger garlic root	Nickle nitrate(0.1n), P.H12 was maintained using NaoH (2n)at 90˚cfor 2h. the precipitates fromed were centrifuged at 10000 rpm for 10min washed with DIA , dried overnight in hot air ovcan at 90˚c,	Ginger 16-52nm Garlic 11-59nm
6	Owolabi Oluwafemi	Sunflower	1:10 (v/v), 10 ml of each plant	42-50nm

	akin kunmi,lawal et.al2022	left	extract was added to100ml of various doses of aeroeous nickle nitrate solution	
7	Ram Krishnan azhagu raj , mohamad s alsathi sandhanasamy devanesam 2017	Coriundram sativum	Ni(No3)2,6H2o as raw material plant dissolved in 500ml of deionized water and strried at 50-60˚c for 45 min.	
8	Lakshmikanth reddy et.al2022	Azadirachta indica(neem)	Nickle nitrate hydroxide (>98.5%) neodymium nitrate hydrate 10gm fresh leaf boiled at a temp of 80 degree c in 100ml of deionized water for 15 min Solution heated at 80˚c for 6 hours.	Avg 96.95nm
9	Tanheeda riaz tayyaba sahzadi et.al2022	Syzygium cumini (jamun)	DPPH (2,2, diphenyl-1 picrylhydrazyl)radical eavnging activity phosphor molydenum complex formation method	10.4 nm
10	p. karpagavinayagam a.emi princess Prasanna c.vedhi et.al2022	Avicennia marina	Ag/Agcl as reference electrode and platinum wire 0.5 m NaoH solution Potential range -0.8 to 1.6 v at scanning rate of 100mvs	40nm

Das et.al 2018, Highly microporous (up to 75%) NiO NPs successfully synthesized by a green route without chemical reductants, pH-invariant and lower overpotential (0.125 V) of O2 reduction on graphite/NiO NPs cathode, Remarkable cell current and efficiency of H2O2 formation (89%) achieved using NiO NPs electrocatalysts, Limiting current density (1.42 A/m2) independent on surface area of graphite/NiO NPs cathodes, Mass transfer coefficient and O2 diffusion layer film found as 0.955×10-5 m/s and 209 µm.

Nkwoada et.al 2021, Green synthesis of reduced graphene oxides provides cost-effective, readily available, and improved material properties. Orange extract-assisted reduced graphene oxide was synthesized by thermal decomposition. The material denoted as o-rGO was characterized via XRD, SEM and FTIR Spectroscopy. Findings confirmed synthesis of o-rGO was successful with interlayer spacing of 2. 98 and crystallite spacing of 0. The adsorption performance of o rGO was investigated over concentrations of Ni2+ in aqueous solution, pH, temperature, and contact time. Removal efficiency of Ni2+ by o-rGO was 97 %

in 10 mins. Thermodynamic parameters demonstrated that the adsorption process was endothermic and non-spontaneous. The findings highlighted the effective green synthesis of reduced graphene oxide for the removal of N12+ ions in aqueous solution. In addition, o-rGO potential for sensors, supercapacitors, and photocatalytic applications can be exploited.

Berede et.al 2024, Te CuO semiconductor catalyst synthesized with a green method was combined with MgAl-LDH and applied for the degradation of MB dye. Te catalytic performance of the CuO/MgAl-LDHs composite exhibited the highest catalytic performance and degraded 99. 20% MB dye within 80 min. However, only 90. 87, and 35. 53% of MB dye degradation was achieved by CuO/MgAl-LDHs , CuO/MgAl-LDHs , CuO NPs, and MgAl-LDHs catalysts, respectively. Te enhanced photocatalytic activity was attributed to a synergistic efect, homogeneous dispersion of CuO NPs, adsorption of MB on MgAl-hydroxyl-rich LDH's structure, and lower band gap of CuO NPs. Te catalyst stability was also checked and 92. 7% of the MB dye removal efciency was still maintained afer fve cycles. Terefore, the CuO/MgAl-LDHs-based photocatalyst could be a potential candidate for the environmental remediation.

Wijaya et.al 2020, GO to RGO by using kafr lime peel extract as a bioreductor was successfully carried out. Te ratio of bioreductor and reduction time has been observed to infuence the characteristics of RGO, and the optimal conditions were found to be 1:2 and 8h, respectively. Analyses of UV-Vis Spectroscopy, FTIR, and XRD indicated the reduction of GO to RGO by the C=C group restoration. Te adsorption study performed on MB showed that the maximum adsorption capacity of RGO was found 276. 06mg/g. MB adsorption by RGO followed pseudo-second-order model; whereas, for the isotherm, the system prefers in line with the Langmuir model. Te RGO-MB adsorption interaction is more dominantly controlled by chemisorption. Te adsorption of RGO-MB was a spontaneous and endothermic process. Te present study indicates RGO prepared by biore duction of RG using kafr lime peels extract a potential adsorbent to remove MB and therefore, it can be further developed for industrial applications.

Bao et.al 2022, The adoption of plant-derived natural products to synthesize metal nanoparticles and their complexes has the advantages of mild reaction conditions, environmental protection, sustainability and simple operation compared with traditional physical or chemical synthesis methods. Herein, silver nanoparticles were in situ synthesized on the surface of graphene oxide by a "one-pot reaction" to prepare graphene

oxide-silver nanoparticles composite based on using AgNO3 as the precursor of AgNPs and gallic acid as the reducing agent and stabilizer. The size and morphology of GO-AgNPs were characterized by ultraviolet-visible spectrophotometer, Fourier transform infrared spectroscopy, transmission electron microscope, X-ray diffractometer and dynamic light scattering. The effects of pH, temperature, time and material ratio on the synthesis of GO-AgNPs were investigated experimentally. The results showed that ideal GO-AgNPs could be prepared under the conditions of pH = 9, 45 C, 2 h and the 2:1 of molar ratio of AgNO3 to GA. The AgNPs within GO-AgNPs are highly crystalline spherical particles with moderate density on the surface of GO, and the size of AgNPs is relatively uniform and determined to be about 8.19 4. 21 nm. The research results will provide new ideas and references for the green synthesis of metal nanoparticles and their complexes using plant derived natural products as the reducing agent and stabilize.

Wardani et.al 2019, nickel Oxide nanoparticles have lived opportunely linked utilizing Ageratum conyzoides L.leaf extract going around green plan. The eye, fundamental, and form of NiO-NP were distinguished. The writing UV-Vis spectrophotometer allowed a typical peak of NiO-NP at maximum instinct of 324 nm. FT-IR writing establishes that the lengthened shuddering of Ni-O takes place at wavenumber of 434 cm 1. The piece intensity dispersal of NiO-NP was 50. 70 91. 3 nm from PSA. The XRD pattern allowed the crystallinity of NiO-NP following having twelve of something inches/30.48 centimeters calculated form. TEM idea presented the mite width of NiO-NP was 8-15 nm. The catalytic exercise allotment of NiO-NP confirmed 83% in the decline of methylene common famous to catalytic project outside inspiration was 28% for 18 outline of conference.

Li et.al 2019, GA-AgNPs were synthesized using a simple and green method. GA-AgNPs inhibited the growth of *Escherichia coli*, Staphylococcus aureus and Candida albicans with MICs of 6, 30 and 24 μg/mL, respectively.GA-AgNPs at the concentration of 6 μg/mL showed no significant cytotoxicity to HL-7702 cells. GA-AgNPs selectively induced apoptosis in HeLa cells.

Jegadeesan et.al 2019, This study presents a facile biogenic synthesis of iron NPs using aqueous extracts of three plant sources: Terminalia bellirica; Moringa oleifera fruit and Moringa oleifera leaves. The total phenolic content was highest for TB extract (3581.36 2. The synthesized Fe NPs were characterized using UV Vis spectroscopy, Fourier Transform Infrared Spectroscopy, Scanning Electron Microscopy, Transmission Electron Microscopy

and X-Ray Diffraction. FT-IR spectra of the extracts and nanosuspensions were similar, with peaks observed at around 3300 3400 cm 1, 1600 cm 1, 1050 1150 cm 1 and 500 cm 1, corresponding to O H, C O, C O and C H stretching, indicating the participation of biomolecules in the nanomaterial synthesis process. TEM and SEM images show single spherical particles for T-Fe, and irregular shaped MOF-Fe and MOL-Fe. XRD analysis confirmed the presence of hematite and ferric oxyhydroxide in the Fe NPs. The antioxidant activity of the aqueous extracts was higher than that of the biogenic Fe NPs, with TB extract the highest among all, given its higher phenolic content. The antimicrobial activity of Fe-NPs was higher than the extract alone, with T-Fe and MOL-Fe the most potent towards S.aureus and B.subtilis. The thermal conductivity of the Fe NPs dispersed in propylene glycol: water base fluid was determined. The high thermal conductivity of Fe NPs in glycol - water mixtures showed its potential as a possible nanofluid for various heat transfer application.

Qiang et.al 2003, This study is to establish optimal conditions for the minimization of iron sludge produced in Fenton oxidation processes by electro-regenerating Fe with constant potential or constant current mode. Results indicate that the optimal cathodic potential for Feregeneration is -0. 1 V vs.the saturated calomel electrode in terms of current efficiency. Keeping the initial Feconcentration]) constant, the average current density produced at -0. SCE is approximately equal to the optimal current density applied in the CCM. The suitable pH range is below the pH value determined by Fehydrolysis. At the optimal potential, the average current density increases linearly with [Fe], exhibiting a slope of 8. The average current efficiency varies with [Fe], e.g., 75% and 96-98% at 100 and > or = 500 mg/L [Fe], respectively. Fe can also be effectively regenerated by dissolving iron sludge at low pH. The unit energy consumption is 2.0-3.

Esquivel et.al 2009, this work is to develop a new TiO2 based photoanode using an optic fiber support. The novel arrangement of a TiO2 layer positioned on top of a surface modified optical fiber substrate, allowed the construction of a photoelectrochemical reactor that works on the basis of an internally illuminated approach. In this way, a semi-conductive optical fiber modified surface was prepared using 30 microm thickness SnO2Sb films on which the photoactive TiO2 layer was electrophoretically deposited. UV light transmission experiments were conducted to evaluate the transmittance along the optical fiber covered with SnO2:Sb and TiO2 showing that 43% of UV light reached the optical fiber tip. With different illumination configurations, it was possible to get an increase in the amount of photo-generated close to 50% as compared to different types of TiO2 films. Finally, the electro-

Fenton photoelectrocatalytic Oxidation process studied in this work was able to achieve total color removal of Azo orange II dye) and a 57% removal of total organic carbon within 60 min of degradation time.

Qin et.al 2019, The non-noble metal.catalysts report a Fe-Co-Ni ternary single-atom catalyst derived from a zeolitic imidazolate frameworks precursor as an efficient oxygen electrocatalyst, and an optimised flexible casting-drying polyvinyl alcohol film as a quasi-solid electrolyte host, for high-efficiency solid-state Zn-air batteries. The aberration-corrected HAADF-STEM and EELS spectrum confirm the co-existence of Fe, Co and Ni single atoms in the FeCoNi-Nx catalyst, and the electrochemical, mechanical, and durability tests prove the superiority of the CD-PVA film. As a result, the FeCoNi-Nx-based rechargeable Zn-air battery delivers superior specific capacity and power density in aqueous electrolyte, as well as an over 60 mW cm 2 power density in quasi-solid electrolyte. As a result, the quasi-solid-state Zn-air battery with a small area of only 2 cm2 is able to charge a mobile phone, which outperforms all the reported devices to date.

Liu et.al 2013, $NaBH_4$ dissolved in EG was used as alkaline precipitant for the first time. $NaBH_4$ dissolved in EG formed a new base macromolecule. The macromolecule was used as alkaline precipitant and structure-directing agent at the same time. NiO was prepared using $NaBH_4$-EG as alkaline precipitant without any templates. NiO synthesized by $NaBH_4$-EG achieved an extremely high specific capacitance of 930 F g^{-1} at 15 A g^{-1}.

Duan et.al2012, NiO nanoparticles with sizes of 3.5 12. 4 nm were grown by thermal decomposing of nickel acetate at different temperatures in NaCl and Li2CO3 alkalisalts. The properties of the nanoparticles were characterized by X-ray diffraction spectrometer, transmission electron microscope, absorption spectrometer, micro-Raman microscope, and superconducting quantum interference device. The effects of the nanoparticle sizes on the crystal structure, exciton ground state energy, vibration modes, and magnetic properties were studied. Lattice parameter of NiO increases with a decrease in nanoparticle sizes. The band gap of NiO nanoparticles increases with a decrease in the nanoparticle size. LO modes of NiO nanoparticles shift red, and the intensity increases with a decrease in the nanoparticle sizes. Bifurcation temperature and blocking temperature of NiO nanoparticles shift to lower temperature with a decrease in nanoparticle sizes.

Shuan et.al 2014, he EFL system, with a Co3O4-graphite composite cathode, degraded the organic dye SRB and persistent organic com-pound 2,4-DCP effectively. The ability of the

EFL system to efficiently generate H2O2 and OH in situ and to cleave the N N bond in SRB are both significant. The Co3O4- graphite composite electrode displays good electrochemical characteristics and produces H2O2 and OH from pH 2 10. The system extends the traditional Fenton reaction pH range and the composite electrode displays high current efficiency. These characteristics give the Co3O4-graphite composite electrode excellent potential in advanced oxidation process-es used to treat water and wastewater containing persistent organic pollutants.

El. Kemary et.al 2013, Nickel group of chemical elements nanoparticles were favorably synthesized apiece response of smaller currency in exchange for larger chloride with hydrazine at range hotness and warm rot of the precursor coat with metallic material hydroxide 2) nanoparticles. The amount were from X-ray diffraction, Transmission energized matter microscopy, Fourier transfer shade resembling such a color spectroscopy, and UV vis absorption spectroscopy. The result of thermogravimetric study presented that the Ni 2 nanoparticles are calcinated at 400 C. The interplays between NiO nanoparticles and level of glucose in blood have existed intentional utilizing UV vis absorption and radiance spectroscopy. The zeta-potential of NiO nanoparticles was used to gain intuitiveness about the interplay mode betwixt NiO nanoparticles and and oxygen.

Chinnaswami et.al 2005, The Ni nanoparticles accompanying fcc or hcp stages have been combined in tetraethylene glycol by utilizing the changed polyol process. The crystal form has happened conditional changing the polyol/Ni blemish percentage and the backlash temperature. The satiation magnetization of the as-groomed pieces depends on the relative volume part of the hcp time. The radioactivity diffraction and lengthened radioactivity incorporation fine structure studies imply the composition of clean fcc and hcp Ni stages. The hcp Ni particles show nonmagnetic presence and thermally fixed beneath 673k.

Brave et.al 2914, Ni2O3 nanomaterial, a aspect of smaller currency in exchange for larger oxide, is combined by a natural synthetic process. The pure natural resources secondhand in the process were coat with metallic material chloride hexahydrate NiCl2.6H2O and potassium hydroxide KOH by utilizing hotness at 250 oC for 2 period. The fundamental, morphological and ocular characteristics of the combined specimens of Ni2O3 were examined engaging various techniques to a degree XRD, AFM, SEM and UV-Vis, individually. The XRD method ratifies the presence of Ni2O3 nanomaterial accompanying clear magnitude of 57.083 nm which indexing to the (2θ) of 31.82; this results told the Ni2O3

was a step of smaller currency in exchange for larger oxide accompanying Nano form. The combined Ni2O3 will be useful in manufacturng electrodes fabrics for fuel container and result catalytic fabrics for electrolysis cell.

Alagiri et.al2012, Nickel group of chemical elements nanoparticles have happened combined in the demeanor of agarose organic compound composed of carbon by brightest star coagulate procedure. The construction, makeup, ocular and attractive possessions of the produce was checked by X-ray dissemination, broadcast power microscopy, UV apparent spectrophotometer and superconducting quantity meddling design magnetometer. The result of thermogravimetric reasoning of the forerunner device demonstrated that the decent calcination hotness was 400 C. X-ray dissemination result told that the got production was coat with metallic material group of chemical elements accompanying face-focused twelve inches/30.48 centimeters measured construction. TEM representation explained that the coat with metallic material group of chemical elements nanoparticles have round shape accompanying proportion about 3 nm. Analysis of FTIR ranges habitual the arrangement of commodity. The ocular incorporation band break of the NiO nanoparticles was supposed expected 3. Magnetic calculation demonstrated that the smaller currency in exchange for larger group of chemical elements nanoparticles exhibit superparamagnetic action at 300 K. Moreover, the nanoparticles show ferromagnetic interplays at 4. 2 K on account of the life of unpaid importance superficial of the nanoparticles.

Rahal et.al 2017, The resultant nanoparticles were characterized by X-ray diffraction (XRD), transmission electron microscopy (TEM), and scanning electron microscopy (SEM). XRD patterns showed that NiO have a face-centered cubic (FCC) structure.The crystallite size, estimated by Scherrer formula, has been found in the range of 28–33 nm. It is noticed that EDTA-capped NiO nanoparticles have a smaller size than pure nanoparticles.Thus, the addition of 0.1M capping agent EDTA can form a nucleation point for nanoparticles growth. The optical and magnetic properties were investigated by Fourier transform infrared spectroscopy (FTIR) and UV-vis absorption spectroscopy (UV) as well as electron paramagnetic resonance (EPR) and magnetization measurements. FTIR spectra indicated the presence of absorption bands in the range of 402– 425 cm−1, which is a common feature of NiO. EPR for NiO nanosized particles was measured at room temperature. An EPR line with g factor ≈1.9–2 is detected for NiO nanoparticles, corresponding to Ni2+ ions.The magnetic hysteresis of NiO nanoparticles showed that EDTA capping recovers the surface magnetization of the nanoparticles.

Senobari et.al 2018, The higher photocatalytic activity of the coupled system relates to its higher charge transfer ability that prevents from the electron/hole recombination. The NiO-CuO catalyst with mole ratio of 1:1 that calcined at 800 °C for 4 h, showed the best photocatalytic activity. The degradation of methylene blue (MB) was followed by UV–vis spectroscopy and the degradation extent was confirmed by chemical oxygen demand (COD) method. To investigate the interaction effects of the experimental variables on the photocatalytic activity of the coupled system, experimental design was applied based on the response surface methodology (RSM) approach. Among the interaction terms, effect of pH- time had the most importance (40%) on the created response. The best MB photodegradation result was obtained in a run included pH 3.5, catalyst dosage of 0.9 g L^{-1}, 3.2 mg L^{-1} of MB during 26 min.

H.chen et.al 2018, Green, facial and rapid Biosynthesis of CuO NPs via ultrasound method using Cystoseira trinodis extracts for first time.Production of the spherical CuO NPs (6–7.8 nm) and antibacterial and DPPH scavenging evolution.CuO NPs with high efficiency(98%) photocatalytic activity for the degradation of methylene blue at pH = 4.

Muthuvel ei.al 2020, Biosynthesis of nanoparticles offered an attractive alternate to chemical synthesis methods. Solanum nigrum leaf aque-ous extract was utilized in the synthesis of metal and metal oxide nanoparticles. The optical bandgap of chemical and biosynthesized CuO-NPs was found to vary from 3.63 to 3.24eV. Copper oxide nanoparticles (CuO-NPs) were synthesized nanoparticles were analysed by XRD, UV–Vis, HR-TEM, DLS, ZE, PL and FT-IR spectroscopy. The X-ray diffraction spectra showed the single-phase monoclinic structure of copper oxide, with an average crystallite size of 2.05–3.00 nm. HR-TEM analysis confirmed the spherical morphology of the synthesized CuO-NPs using chemical and biological methods with an average size of 32 nm and 25 nm, respectively. The synthesized CuO-NPs exhibited potential photocatalytic activity towards the degradation of methylene blue dye on exposing to sunlight irradiation. The degradation effectiveness against methylene blue dye was found to be 85 and 97% for chemical and biosynthesized CuO-NPs, respectively.

Zelekew et.al 2017, The NiO/NiS composite motivation combination is devised utilizing a plain and easy order. Composite matters accompanying various sulfur beginnings were distinguished and used for catalytic decline of 4-nitrophenol in liquid resolution. The incentives' recognition towards decline/decolorization of different basic dyes in the way that

methylene vulgar , methyl cantaloupe , and rhodamine B was judged. The NiO/NiS composite incentive planned accompanying 10 mmol of Ni 2 4H2O and 5 mmol of thioacetamide had best choice catalytic project and the catalytic decline of 4-nitrophenol to 4-aminophenol accepted only 6 brief time period. The composite stimulant still acted yes for decline of MB, MO, RhB, and a combination of basic contaminants containing 4-NP, MB, MO, and RhB, that were achieved in 60, 30, 90, and 210 s, individually.

Manjari et.al 2017, CuO nanoparticles (NPs) utilizing environmentally mild and sustainable sources, outside the need for synthetic lowering and stabilizing powers, is stated in this place study. Aqueous extract of A. elaeagnoidea flowers serves as the reducing, completing, and securing power in this green combining approach. Remarkably,The CuO NPs formed have a content grazing from 20 to 45 nm. After combining, they can be divided by way of centrifugation and reused for six phases with over 90% adaptation adeptness. This focal points the efficiency and influence of the green combining form in producing CuO NPs accompanying advantageous features for industrial uses, further stressing allure potential for large-scale combining and arrangement across miscellaneous sectors.

Inocencio et.al 2021 Foresee advanced and innovative strategies is a key approach and constitutes a cornerstone for accessing clean, affordable, and reliable energy to satisfy the world's increasing prosperity and economic growth. To this end, hydrogen energy technologies parade as promising sustainable solutions to the looming energy crisis at either the small or large industrial scale, Water electrolysis with renewable energy is one of the best solutions to produce hydrogen without COx emissions. However, the practical realization of this elegant opportunity of paramount importance is facing several challenges, among which are: the efficient design of cathode and anode catalytic materials exhibiting improved intrinsic and durable activity; the scale-up of the system for the large-scale hydrogen production through the electrochemical water splitting. This review puts these opportunities and challenges into a broad context, discusses the recent research and technological advances, and finally provides several pathways and guidelines that could inspire the development of ground breaking electrochemical devices for hydrogen production.

Table -2

Reference	Metal Oxide involved	Electrodes	electrolyzer	NOTES	Optimal Structure or Configuration	Illumination Source	Electrolyte	Other Electrodes	Hydrogen Evolution Rate	current conversion efficiency	hydrogen efficiency
Hadia .et.al 2023	graphene	CuFeO2/ CuO/Cu		immersed in 0.05 M FeCl3 for 15 min on each side and dried at 60 ◦C for 2 h. combusting the substrate at 500 ◦C for 10 min	sewage water with a pH of 7.2. A 400 W metal halide lamp (light intensity) with a photon flux of 500 µmol/s	400 W metal halide lamp at a sweep rate of 1 mV/s and a temperature of 25 ◦C	Sewage water	Graphite / calomel	90 µmol/h	Jph 0.45 to −0.79 mA·cm −2 Particle size- 390 to 640 nm Ph=7.6	88%
Xie, et.al 2022	Molten salt	LiH on the Ni wire Mo rod (D: 12		----	----	performing cyclic voltammetry using molten	---	----		1.5 V at 660 ◦C using a DC power supply	83.2 %

		mm)cathode				lithium chloride as the electrolyte at 660 ◦C under a flow of moisturized argon.					
Gürünlü et.al2020	graphene	graphite		Using hammers method Produce RGO powder	molten salt mixture of LiCl-KCl			(GGr500, GGr600, GGr700, and GGr800)		284.24, 286.28, 290.37, and 285.02 eV 40mA Particle size=275 to 285 nm 600 dergee c	86%
Zhu et.al2020	Metal oxide	HER catalyst Co3O4 Co-MOF		0.5 M H2SO4 solution			1 M KOH solution	Co, Ni, Fe, Mn Pt		138mV at 10mA Ph=universal Particle size 20-40 nm	

Park et.al 2021	Metal oxide	anode BDD@TiC NAs cathode Pt@C @TiC NAs		0.5 m H2So4 soluation 0.1 Na2So4 aqucous soluation	degradation of benzoic acid, sulfate radical generation, and hydrogen production				40µmol/h Constant voltage 4.5v Ph= 6.5 680 ——————— C	5 to 10nm	
Rabia et.al 2022	graphene	PMT/roll-GO Counter electrode calomel and graphite	PEM	200 µL of graphene solution is drop-casting over the PMT thin film. Then, PMT/roll-GO is dried at 70——— C for 30 minutes		xenon lamp	6 g KMnO4		10 µmol/h cm	2.67eV 0.078 – 0.295mA At 20 to 60 dergee Particle size-636nm Ph=4	
Sameerah I. Al-Saeedi Et.al 2023		ZnO Nanorod-arrayed electrode		(0.05 M) solution of zinc acetate dihydrate, Zn(CH3COOH)·2H2O, with (HMT, 0.05 M) dissolved in 20 mL of deionized water (DI) water at 80 ◦C		monochromatic light	0.5 M Na2SO3·7H2O		28.43 mmol h −1 cm−2	0.77 mA/cm2 @1 V Particle size-42.1nm	87.4 %

				After 20 min of continuous stirring ph 6.6 using 0.1 M NaOH solution and the deposition was carried out for 2 h then dried room temperature.							
Eidsvåg et.al 2021	n-doped metal	TiO2	PEM			Solar panel UV light	MOS2 or WS2		49.2 µmol/h cm	2.90 mA/cm2 2.15 eV	49.2
Mostafa et.al2022	AlO3	Graphite calomel	PEM	C2H5OH: HClO4 (1v:1v) solution oil pressing machine for 3 min at 10 kN/cm2, 99.99% of the imprinted aluminum foil was produced ethylene glycol:H3PO4: H2O (100v:1v:200v) took conducted at 2 ◦C for 15 and 120 min mixture of H3PO4 (6 wt.%) and H2CrO4 (1.5 wt.%) for 12 h at 60 ◦C. Lastly, to complete Al2O3 synthesis, the pore siding is carried out using 6 wt.%		xenon lamp monochromatic light	Sewage water	Ag2O-Ag/Au/Al2O3		9.5mAcm-2 1.56 eV Particle size-29.6nm	30%

Table -3

SL NO	REVIEW PAPER SOURCE	TYPES OF electrode & catalyst	RESULT	PARTICLE SIZE
1	Cheng Wang, Hongyuan Shang, Liujun Jin et.al 2020	Fe-Co2P NiRuIr/G Mn–NiO–Ni/Ni–F NiCoN|NixP|NiCoN PtRuMo Co3Mo3C/CNT U-CNT-900 Rh/N, S-copded carbon Mo5N6 nanosheets Ni5P4@Ni2+δOδ(OH)2−δ NiCoP	489mV 80mV 170mV 165mV 196mV 10mA 124mV 250mV 320 mV 257 mV 144 mV 287 mV 1.23 V(overall) (pH = 7.8)	
2	Kaiyu Xie , Ali Reza Kamali Et.al 2022	s platinum (Pt), iridium oxide (IrO2) and ruthenium oxide (RuO2)	1.5 v 660 ◦C	
3	Jonathan Mbah a , Eric Weaver b , Sesha Srinivasan c,*, Burton Krakow b , John Wolan b , Yogi Goswami b Et.al 2010	ruthenium oxide (RuO2) coated silicon (Si)	0.5v to 1.23v Upto 500 drgee C	
4	Betül Gürünlü , Çiğdem Taşdelen Yücedağ, and Mahmut Rahim Bayramoğlu Et.al2020	Green synthesis graphene from graphite	Ph 6, 40mA 600° C to800° C	0.34 nm RGO synthesized byHummer's method was found to be 738 nm
5	N. M. A. Hadia 1,2 , Mohamed Shaban 3,4 , Ashour M. Ahmed 4,5, W. S. Mohamed 1 , Meshal Alzaid 1 , Et.al2021	CuFeO2/CuO/Cu	0.45 to −0.79 mA·cm−2 0.7 to 1.6 eV, 100–300 ◦C	640 to 390 nm
6	Yinlong Zhu, *a Qian Lin,a Yijun Zhong,b Hassan A. Tahini, c Zongping Shao bd and Huanting Wang * Et.al2020	metal oxide-based HER pt	20 mV at 10 mA cm2	
7	Sung-Woo Park,‡a Eun-Tae Yun,‡a	Pt plate BDD@TiC	1.23v 1.3 and 2.5 V	——— 100 nm

	Hyun Jung Shin,a Wooyul Kim, b Jaesang Leea and Dong-Wan Kim Et.al 2021		Upto 900 degree c	5–10 nm
8	Carlos V. M. Inocêncio1 Yaovi Holade2 Claudia Morais1 K. Boniface Kokoh1 Teko W. Napporn1 Et.al 2021	OER and HER catalysts Electrode (RHE)	1.23 V at 25°C and 1 bar −0.059 pH 120.2 mV/de	
9	Francesco Zaccaria et.al 2021	[FeFe], [FeNi] or Fe hydrogenase enzymes	pH = 7, 430mV	
10	Tahiraet.al 2020	Metal oxide Pt, Ir, and Ru	31 mV	
11	Mohamed Rabia1,2 | N. M. A. Hadia3,4 |Mohamed7,8 | Mohamed Shaban Et.al 2022	poly(m-toluidine) (PMT)/rolled graphene oxide (roll-GO	m 0.078 to 0.295 mA.cm2 1.65, 2.38, and 2.67 eV 20C to 60C	390 to 636 nm
12	Sameerah I. Al-Saeed Et.al 2023	ZnO	3.27 eV to 2.99 eV 63.7 and 87.91 mV <100 drgee c	42.1 nm 390 nm and 636 nm
13	Tamanna Islam 1,† , Md. Mahedi Hasan 1,† , Abdul Awal 1 , Md Nurunnabi 2,3,4,* and A. J. Saleh Ahammad et.al 2020	MNP-graphene nanocomposite (AuNPs), silver (AgNPs), and platinum NPs (PtNPs)	0.7 V	1 and 100 nm
14	Håkon Eidsvåg 1,* , Said Bentouba 1 , Ponniah Vajeeston 2 , Shivatharsiny Yohi 3 and Dhayalan Velauthapillai et.al 2021	TiO2	1.6–3.2 eV	11–35 nm
15	Huda Mostafa 1,2, Ashour M. Ahmed 2,3, Mohamed Shaban 2,4 , Ahmed A. Abdel-Khaliek 1 , Fuead Hasan 5 , Fatimah Mohammed Alzahrani 6,* and Mohamed Rabia et.al 2022	(Ag2O-Ag/Au/Al2O3)	8.9 to 9.5 $mA.cm^{-2}$. 25 to 75 $mW.cm^{-2}$ 400 ◦C for 2 h	350nm

16	Joseph P. Torellaa,1, Christopher J. Gagliardib,1, Janice S. Chena , D. Kwabena Bediakob , Brendan Colóna , Jeffery C. Wayc , Pamela A. Silvera , and Daniel G. Nocerab,et.al2014	NiMoZn	pH=6-8 2.5 V 0.5 and 11 mA/cm^2 .	
17	Jiayi Li1,2,§, Xin Mao3,§, Wanbing Gong1 (ʊ), Xinyu Wang1et.al 2020	Ni-Co2P	1.53 V 10 mA·cm−2, 250mA 350 drgee c	532nm

3. Experimental chemicals, Materials and method

3.1. Chemicals and Reagent

It seems like you're providing information about the chemicals used in a experiments. Here's mentioned that's chemicals. **Nickel sulphate heptahydrate (NiSO4.7H2O)** This compound, with an assay range of 97-104%, is used as the precursor for generating nickel oxide (NiO) nanoparticles (NPs). It's likely used for its nickel content and solubility in water. **Na2SO4 (Sodium sulfate)** an assay of at least 99%, is used as the supporting electrolyte (SE) in the experimental setup. Sodium sulfate is commonly used in electrolyte solutions due to its high solubility and ability to conduct electricity. **KBr (Potassium bromide)**: With a minimum assay of 99.5%, potassium bromide may be used as a supporting reagent or as part of the experimental setup for specific reactions or analyses. It's often used in various laboratory processes **Ethanol** with an assay of 98%, is a common solvent used in laboratories. It may be used for dissolving or diluting certain substances during the experimental procedure. **H2SO4 (Sulfuric acid)**: With an assay range of 95-98%, sulfuric acid is a strong mineral acid used in various laboratory applications, such as adjusting pH, preparing solutions, or catalyzing reaction. **NaOH (Sodium hydroxide)** assay of 98%, sodium hydroxide is a strong base often used in laboratory settings for pH adjustments, neutralizations, or as a reactant in chemical reactions. **H2O2 (Hydrogen peroxide)** assay of 30%, hydrogen peroxide is used as a reagent in the experimental procedures, likely for its role in H2O2 generation or as a standard solution for calibration purposes. **Acetonitrile** This solvent assay of 99.5%, is obtained from LOBA Chemie and may be used in various aspects of the experimental setup, such as solvent extraction or as a mobile phase in chromatographic analyses. **Graphite powder** a particle size of less than 20 µm, is sourced from Sigma Aldrich and used for fabricating electrodes. Graphite is commonly used as an electrode material due to its conductivity and stability. **Paraffin wax** This material is obtained from LOBA Chemie and is used in the fabrication of electrodes, likely as a binder or insulating material in electrode construction. **Nafion** a perfluorosulfonic acid-PTFE copolymer in a 5% w/w solution, is used as a binder to embed NiO nanoparticles (NPs) onto the surface of the working electrode (WE). Nafion is known for its ability to facilitate electrode immobilization and improve stability. **TiO2 (Titanium dioxide)** assay of at least 99% from Sigma Aldrich is used to prepare titanic sulfate reagent. This reagent is employed for determining hydrogen peroxide (H2O2) concentration, likely through a colorimetric or titration-based method. **Deionized water** is used for preparing reagents, solutions, electrode washing, and other laboratory procedures. These all materials and chemicals are essential components in the experimental setup for synthesizing NiO

nanoparticles, fabricating electrodes, and conducting analyses related to H2O2 generation and determination. All chemicals and reagents except DI water purchased from Kolkata, india[1,2,3].

3.2. Preparation of bio-extract

The properties of orange and 150g per was collected from the station market near jadavpur university Kolkata west Bengal India. It was first washed in our lab running tap water and then in distilled water. The peel was removed, and the flesh was cut into small pieces (6 mm × 4 mm × 2 mm). The extraction experiment was carried out in a conical vessel of 500 mL with 100 g pieces in 300 mL deionized water and boiled it for 12 hr at 85-90ºC with stirring at 400 rpm on a magnetic stirrer (Tarsons Products Pvt. Ltd., Kolkata, India) for the extraction of analytes. The bio-extract after reaching room temperature was filtered out using 2 μm glass fiber filter paper (Prefilter AP25, Millipore, Germany) and, a typical volume of 390 mL bio-extract (pH 5-6) was collected. The clear filtrate (termed as bio-extract) was a slightly yellow color, and it was prepared freshly before every synthesis experiment [2,3].

3.3. NiO NPs synthesis methodology

In a typical experiment, an equal volume of 50 mM NiSO4 (pH ~3.85) and asprepared bio-extract was mixed by vigorous stirring (300 rpm) for 10 min. pH of this mixture was increased from 4.65 to 11 by drop-wise addition of 2 M NaOH. The residue after 48 h of continuous stirring at 65-70 ºC was cooled down to room temperature and, collected by centrifugation at 4000 rpm for 5 min (K 70, REMI Instruments Ltd., India). It was then dispersed in deionized water-ethanol solution (30:70 %) and sonicated for 10 min (50 Hz, Jeio Tech Co. Ltd., Seol, Korea) and, the residue was recovered by centrifugation as stated before. This procedure was repeated thrice to eliminate uncoordinated biomolecules present in the residue [30,37]. The so called clean residue was dried (termed as Ni-dry) at 95 ºC in a hot air oven (ROV/DG, Reico Equipment and Instrument Pvt. Ltd., Kolkata, India) and, then calcined at 500 ºC for a period 2 h [38] in a muffle furnace (LEF-115P-2, Daihan Labtech Co., Ltd., Namyanglu-City, South Korea) for the formation of NiO NPs. The experimental steps for the synthesis of NiO NPs are schematized in Fig. S2 of the Supplementary Material. In the case of control experiment (termed as Ni-control), the same procedure was followed, however, without the use of bio-extract/analytes. NiO NPs were also prepared using commercial AA of 10 mM [15,39] instead of using the bio-extract without changing other experimental condition [2].

3.4. Electrochemical studies

3.4.1. Fabrication NiO NPs embedment support on graphite

The meticulous fabrication process for the graphite support-electrode was executed with utmost precision to guarantee optimal quality. Initially, a carefully measured mixture consisting of 3.75 grams of graphite powder and 2.25 grams of paraffin wax was meticulously blended at a controlled temperature range of 60-70 ℃ for a specific duration of 15-20 minutes. Following this meticulous blending step, the homogeneous composition was cautiously poured into a precisely measured rectangular wooden mould measuring 55 mm × 8 mm × 4 mm to give the electrode its defined shape, as visually demonstrated in Fig. S3a of the Supplementary Material. An integral part of this process involved the insertion of a high-quality copper wire, with a diameter of 1 mm and a remarkable electrical conductivity value of 5.96×107 S/m at 20 °C, into the mould to establish the necessary electrical connection for the electrode. Subsequently, the composite of graphite and paraffin underwent a gradual solidification process, cooling down slowly to room temperature before being meticulously extracted from the mould, confirming its essential role as the graphite foundation for the electrode's support structure. During the electrode modification phase, a meticulous and precise approach was also adopted. Initially, a specific quantity of 10 milligrams of NiO nanoparticles was carefully dispersed in 1 milliliter of a 0.5% Nafion solution and then subjected to thorough mixing through sonication at a precise frequency of 40 kHz for a controlled duration of 2 hours. Following this meticulous mixing process, the resulting suspension was effectively applied using a brush-coating technique onto the surface of the graphite electrode, resulting in the creation of the composite graphite/NiO nanoparticles electrode.

The modified electrode was then left to undergo a meticulous drying period at ambient temperature for 12 hours before being gently cleansed with deionized water and air-dried, as extensively elucidated in the Supplementary Material. It is important to emphasize that the same intricate procedure was consistently replicated for the electrode modifications utilizing the Ni-control method (referred to as the graphite/Ni-control electrode) and the Ni-dry particles (referred to as the graphite/Ni-dry electrode), ensuring a high level of methodological coherence and conformity throughout the entirety of the electrode fabrication process.

3.4.2. Electroanalytical methods

The detailed experimental setup described in the study meticulously outlined the methodology employed for investigating the electrochemical behavior related to the generation of hydrogen peroxide (H2O2) using the cyclic voltammetric (CV) technique. The experimental configuration included critical elements such as advanced equipment utilization, encompassing a high precision potentiostat/galvanostat from AUTOLAB 302N, Metrohm Autolab B.V, Netherlands, which played an instrumental role in controlling and measuring the electrochemical processes with utmost accuracy.the electrode system applied in the study consisted of a sophisticated three-electrode setup, featuring a working electrode (WE) crafted from various materials such as graphite, graphite/Ni-control, graphite/Ni-dry, or graphite/NiO NPs (nanoparticles), a platinum (Pt) counter electrode with a 2 mm diameter, and an Ag/AgCl (3 M KCl) reference electrode. This configuration facilitated precise control and thorough measurement of the electrochemical reactions under evaluation.the experimental setup, the electrolyte solution used during the experiments was accommodated within a 220 mL electrochemical cell, supplemented with 190 mL of a supporting electrolyte (SE) solution. The SE solution comprised 0.5 M Na2SO4 with pH levels adjusted to acidic conditions between 1.5 and 4.5 through the utilization of a dilute H2SO4 solution (0.5 M), thereby creating a conducive environment for the desired electrochemical responses. the process involved a pre-experiment step of oxygen purging, wherein O2 (99.99% purity) was introduced into the cell at a controlled flow rate of 1.0 LPM for a duration of 20 minutes. This crucial preparatory measure ensured the establishment of a stable oxygen-rich environment necessary for the ensuing electrochemical reactions.The optimization of scan rates for the cyclic voltammetry (CV) tests, ranging from 1 to 200 mV s-1, was complemented by the corresponding adjustments in pH levels of the supporting electrolyte solution, aligning the experimental conditions meticulously to the research objectives. Furthermore, the study conducted an amperometric test over a designated 2-hour timeframe to evaluate H2O2 formation using a fixed potential (-Ecat) of 0.268 V vs. Ag/AgCl, derived from prior CV assessments conducted with the graphite/NiO NPs working electrode. Lastly, the calculation of the current efficiency (CEf) for H2O2 production was an essential metric determined by quantifying the electrical current essential for H2O2 generation relative to the total current passing through the cell, contributing vital insights into the efficiency and behavior of the studied electrochemical process under the controlled experimental conditions outlined[4,5].

$$CE_f = \frac{nF C_{H_2O_2} 2}{\int_0^1 Idt} \times 100, \%$$

[4]

where, n = stoichiometric number of electrons transfer for H2O2 formation, F = Faraday's constant (96485 C/mol), = mole of H2O2 formed, I= cell current (A) supplied for the time period of t (s). Here, it is important to mention that the rate of H2O2 formation is governed by the DO transport from the bulk to the WE surface [5].

4. Solar-Driven Hydrogen Production

The hydrogen production is sourced from four primary sources, namely natural gas, coal, oil, and electrolysis. Among these sources, steam reforming accounts for a significant portion, making up 48% of the world's total hydrogen production. Coal follows with an 18% contribution, whereas oil and electrolysis represent 30% and 4%, respectively. The conventional methods of hydrogen production from natural gas, coal, and oil are marked by high energy consumption and dependence on non-renewable resources, a situation that raises concerns regarding environmental conservation and climate change mitigation efforts. In contrast, electrolysis offers an environmentally friendly approach to hydrogen generation, relying solely on water and an electrical current. To transition towards greener hydrogen production methods, it is suggested to leverage renewable energy sources such as wind, hydro, and solar power to supply the necessary electricity for water electrolysis. Solar power emerges as particularly advantageous due to its abundant energy potential. Various techniques are utilized in the electrolysis process, including thermochemical water splitting, photo-biological water splitting, and photocatalytic water splitting. Among these methods, photocatalytic water splitting is highly favored due to its exceptional solar hydrogen conversion efficiency, cost-effectiveness, and the ease of separating oxygen and hydrogen during the operation. This approach allows for the flexibility of implementing hydrogen electrolysis across a spectrum of applications, ranging from small-scale installations to large industrial facilities.

4.1. Hydrogen production technologies

The hydrogen sector consists of four main segments: production, storage, transportation, and utilization. Within these sectors, natural gas serves as the predominant source for hydrogen production, whereas the ammonia industry stands out as the largest consumer of hydrogen. Effective and efficient transportation of hydrogen between production and consumption sites

plays a crucial role in the overall economics of hydrogen production. This process is essential for managing production costs and ultimately impacts the accessibility and affordability of hydrogen. Through the illustration below, it is evident that ensuring a smooth and cost-effective transition of hydrogen from where it is produced to where it is needed is integral to the success and sustainability of hydrogen-based economies.

Hydrogen storage is widely acknowledged as a critical and complex phase in the development of secure, dependable, efficient, and sufficient storage methods (Zhang et al., 2016). Consequently, there have been suggestions for hydrogen production procedures grounded on raw materials. In this context, provides a concise overview of the various hydrogen production techniques, with particular attention drawn to water electrolysis. This process involves the decomposition of water into hydrogen and oxygen through the application of an electric current. It is imperative to explore efficient and cost-effective methods.

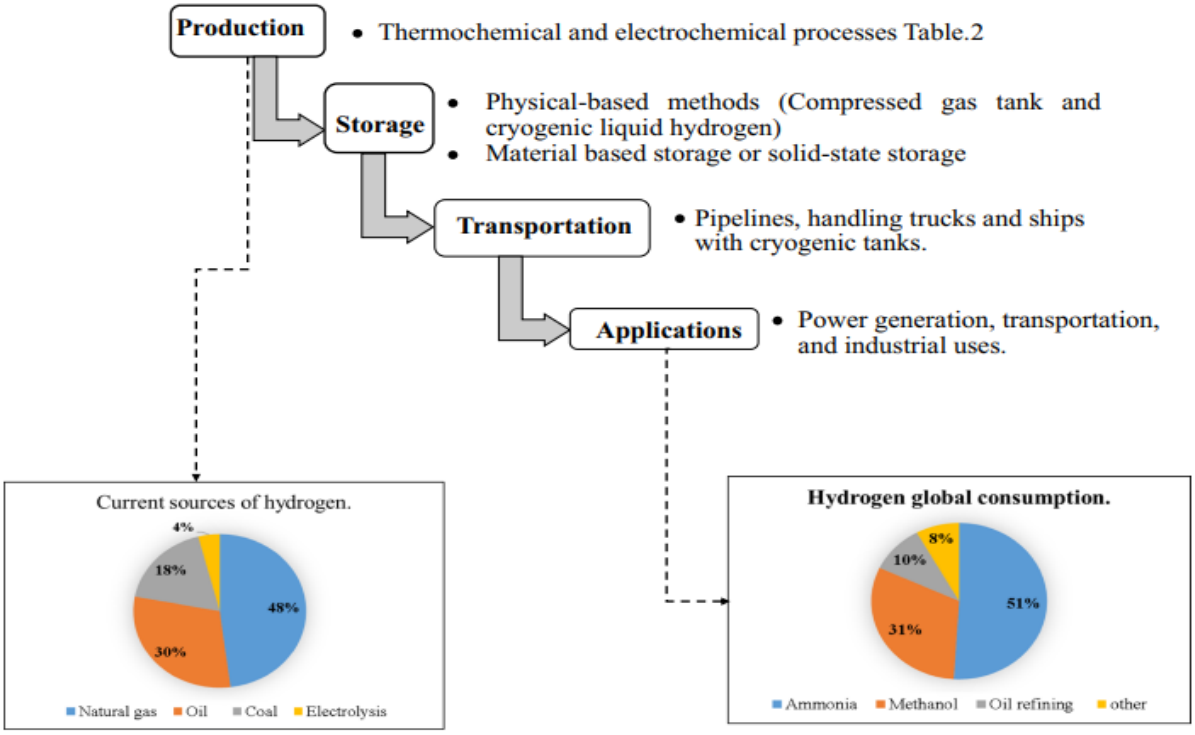


Fig. Stages of the hydrogen industry (Arregi et al. 2018; Abohamzeh et al. 2021).

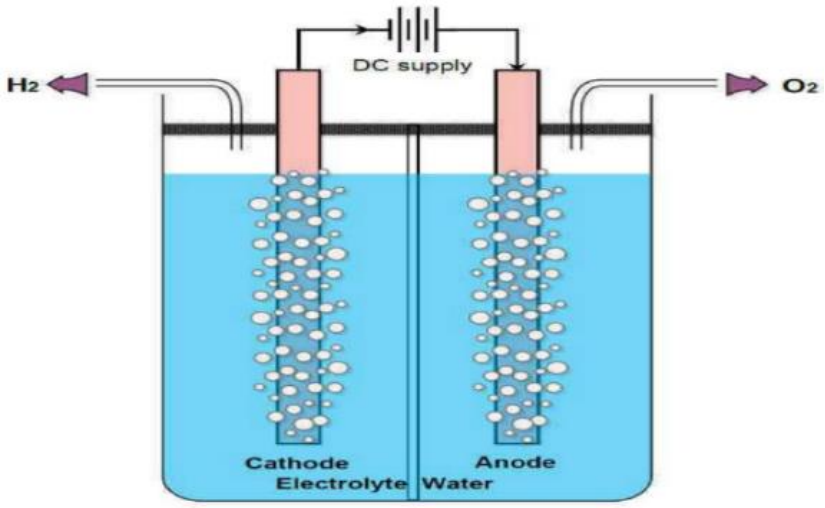
Hydrogen has a low carbon footprint. It could thus significantly reduce energy-related CO_2 emissions and help limit climate change. Fuel cell electric vehicles (FCEVs) can provide the mobility service of today's conventional cars with potentially very low carbon emissions. Although the potential benefits of hydrogen and fuel cells in end-use applications are promising in terms of environment and energy security, the development of hydrogen production,

5. Water electrolyzer

Two essential components of a green hydrogen system are its renewable energy source and the use of a water electrolyzer. This electrolyzer plays a crucial role in the process by breaking down water into its elemental components of hydrogen and oxygen when electricity is applied, giving it a pivotal position within the hydrogen production cycle. Despite occasional interruptions in its operation due to intermittency, the electrolyzer stands out as a highly viable and commercially attractive means for generating hydrogen and storing energy, especially when integrated with renewable energy sources like solar, wind, and biomass.

The electrolysis of water emerges as a standout method for hydrogen production due to its sustainable use of H2O, resulting in the production of only pure oxygen as a by-product. Noteworthy is the fact that the electrolysis process draws on direct current (DC) power harnessed from renewable energy sources, aligning it strongly with global efforts to transition towards sustainable energy solutions. It is worth highlighting that currently, only a fraction of hydrogen production, approximately 4%, is obtained through water electrolysis largely due to economic constraints. This percentage is expected to rise significantly in the future with the anticipated increase in the adoption of renewable energy sources, like solar, wind, and nuclear, as outlined by the European Energy Directive aiming to source 14% of energy requirements from renewable sources by 2020, with a target of 30% by 2030 in India. Moreover, the benefits of water electrolysis are manifold, showcasing high cell efficiency and a heightened rate of hydrogen production coupled with exceptional purity levels. These advantages set the stage for further conversion of hydrogen into electrical energy using low-temperature fuel cells, accentuating the versatile nature of hydrogen as an energy carrier. In delving deeper into the electrolysis process, water molecules serve as the primary reactant, undergoing dissociation into hydrogen (H2) and oxygen (O2) under the electrically induced decomposition. Water electrolysis can be delineated into four distinct categories based on varying electrolytes, operational conditions, and the roles of ionic agents (OH, H+, O2), albeit with consistent underlying operating principles governing each classification.Two essential components that play a crucial role in the functioning of a green hydrogen system

are its renewable energy source and the utilization of a water electrolyzer. The process of water electrolysis, wherein water breaks down into hydrogen and oxygen when an electrolyzer is operated with electricity, signifies a significant advancement in sustainable energy production. This specific electrolyzer, due to its intermittent operation, has emerged as a highly viable and commercially feasible approach for hydrogen generation and energy storage, especially when integrated with renewable energy sources. Notably, the various types of electrolyzers available, such as the proton exchange membrane electrolyzer (PEM), alkaline water electrolyzer (AWE), alkaline anion exchange membrane (AEM), and solid oxide electrolyzer (SOE), each offer distinct advantages and features as outlined in Table 3. The advantages of employing renewable energy in conjunction with water electrolyzers are numerous, including the potential reduction or elimination of transportation and storage expenses by deploying stand-alone systems at end-user facilities. Moreover, the compactness of these systems and their ability to achieve high levels of hydrogen production compared to photo-electrochemical methods make them highly attractive for various applications. An additional benefit lies in the fact that these systems eliminate the need for extensive electricity infrastructure, particularly in arid regions, making them a viable option for sustainable energy solutions. Adding to their appeal is the fact that they are readily available in the commercial market (Nasser et al., 2022a). When considering the composition of electrolyzer stacks, they consist of multiple interconnected cells that can be broadly categorized as monopolar or bipolar types. The bipolar design, which connects the cells in series, offers advantages in terms of space efficiency and reduced electric wiring requirements compared to monopolar configurations. However, the higher cost associated with the complex design of bipolar stacks poses a significant challenge to their widespread adoption (Zhang et al., 2016).



5.1. Principle of water electrolysis

Water electrolysis is the process whereby water is split into hydrogen and oxygen through the application of electrical energy, as in Eq. (6). Typically, a water electrolysis unit consists of an anode, a cathode separated with an electrolyte, and a power supply. The electrolyte can be made of an aqueous solution containing ions, a proton exchange membrane (PEM) or an oxygen ion exchange ceramic membrane. A direct current (DC) is applied from the negative terminal of the DC source to the cathode (seat of the reduction reaction), where the hydrogen is produced. At the anode, the electrons produced by the electrochemical reaction return to the positive terminal of the DC source.

For the case of water electrolysis in an acid aqueous electrolyte, the processes that occur at the anode and the cathode are described, respectively, [51] by Eqs. 1 and 2:

$$H_2O \rightarrow \frac{1}{2}O_2 + 2H^+ + 2e^- \qquad E^{\circ}_{H_2O/O_2} = 1.23V/ENH \qquad 1$$

$$2H^+ + 2e^- \rightarrow H_2 \qquad E^{\circ}_{H^+/H_2} = 0.00V/ENH \qquad 2$$

The half reactions occurring on the cathode and anode, respectively, can be written as:

$$2H_2O + 2e^- \rightarrow H_2 + 2OH^- \qquad E^{\circ}_{H_2O/H_2} = -0.83V/ENH \qquad 3$$

$$2OH^- \rightarrow \frac{1}{2}O_2 \rightarrow H_2 + 2OH^- \qquad E^{\circ}_{H_2O/H_2} = -0.83V/ENH \qquad 4$$

The global reaction for the two cases is:

$$H_2O \rightarrow H_2\,\frac{1}{2}O_2 \qquad \Delta E^0 = E^{\circ}_{H_2O/H_2} - E^0_{\frac{OH^-}{O_2}} = -1.23V \qquad 5$$

Electrolysis of water is not a spontaneous phenomenon because the standard global reaction potential is negative.[50,52] Therefore, it needs an external intervention (power source) and the global reaction can be written as:

$$H_2O + Electricity \rightarrow H_2\,\frac{1}{2}O_2 \qquad 6$$

5.2. Thermodynamic

The equation of the German chemist Walther Nernst can be obtained from thermodynamics. The variation of Gibbs free energy is a function of the concentrations of the species participating in a chemical reaction ($aA + bB + \cdots \rightarrow mM + nN$ ...)

$$\Delta G = \Delta G^{\circ} + RT.\ln\left(\frac{a_M^m.a_N^n}{a_A^a.a_B^b}\ldots.\right) \qquad 7$$

where $a_A^a.a_B^b$ …. $a_M^m.a_N^n$……..are the activities of the species.

The Nernst equation is a fundamental equation in electrochemistry that relates the electrode potential of an electrochemical cell to the concentrations (or activities) of the species involved in the cell reaction. It's particularly important for understanding how the cell potential changes with varying concentrations of reactants and products.[50]

The equation is often written in the form:

$$\Delta E_{npile} = \left(E^{\circ}_{cathode} - E^{\circ}_{anode}\right) - \frac{RT}{nF}\ln\left(\frac{a_M^m . a_N^n}{a_A^a . a_B^b}\right) \quad 8$$

5.3. Faraday's law

In 1832, Michael Faraday stated his two laws of electrolysis:

1. The weights of substances formed at an electrode during electrolysis are directly proportional to the quantity of electricity that passes through the electrolyte.

2. The weights of different substances formed by the passage of the same quantity of electricity are proportional to the equivalent weight of each substance.

Faraday's law of electrolysis quite accurately. expresses the relationship between the mass of material deposited or produced during electrolysis (*m*), the proportionality constant (*k*), the instantaneous current flowing through the cell (*I*), and the duration of electrolysis (*t*).

$$m = k . \int_0^t I . \, dt \quad 9$$

The relationship can also be expressed in terms of Faraday's constant (*F*), the molar mass of the substance (*MM*), the number of exchanged electrons (*n*), and the quantity of electricity (*Q*):

$$\mathrm{m} = \frac{I.t.M}{nF} \quad 10$$

In this equation:

- *m* is the mass of the substance formed or deposited (measured in grams).
- *I* is the current flowing through the cell (measured in amperes, A).
- *t* is the duration of electrolysis (measured in seconds, s).
- *M* is the molar mass of the substance formed (measured in grams per mole, g/mol).
- *n* is the number of exchanged electrons in the reaction.
- *F* is Faraday's constant (measured in coulombs per mole of electrons, C/mol).

This equation shows how the mass of a substance produced during electrolysis is directly proportional to the current, time, and molar mass of the substance, while also relating these factors to the fundamental properties of electricity and electron exchange.

6. Types of Electrolyzer

6.1. Proton exchange membrane electrolyzer (PEM)

It is evident that discussions are heavily focused on the revolutionary PEM electrolyzer technology, a method employed in the generation of hydrogen. The inception of the PEM electrolyzer can be traced back to the 1960s, marking a significant milestone when General Electric first introduced this groundbreaking technology. This pioneering innovation heralded a new era in hydrogen production methods by introducing a device consisting of essential components – the anode, cathode, and electrolyte – which were pivotal for its operation and functionality. The utilization of precious materials like platinum, iridium, ruthenium, and platinum on carbon has long been the norm in constructing the anode and cathode segments of the PEM electrolyzer, ensuring optimal efficiency and performance.

In the present market landscape, two key players in the field of PEM membranes have emerged – The Chemours Company FC, LLC, known for its renowned Nafion trademark, and FUMATECH BWT GmbH, distinguished for its Fumapem trademark. These specialized membranes play a crucial role in enhancing proton conductivity, reducing gas crossover, enabling a compact design, and supporting operation under high pressures ranging from 15 to 30 bar at temperatures between 50 to 90 degrees Celsius. The PEM electrolyzers come with a plethora of benefits, including their exceptional adaptability to varying load demands and their ability to produce hydrogen of extraordinary purity levels reaching up to 99.999%. Nonetheless, a significant hurdle that has persisted in the realm of PEM electrolyzers is their relatively high production costs attributed to the incorporation of noble materials in their manufacturing process.Immersing oneself in the detailed insights found in Table 3 would provide a comprehensive understanding of the operational principles and key performance parameters governing PEM electrolyzers. These valuable data shed light on the inner workings of these electrochemical devices, allowing for a deeper appreciation of their efficiency and efficacy in the spheres of hydrogen production and fuel cell technology advancement.[40,43]

aElectricity is produced from renewable energy sources, grid, or energy recovery

bThe electrolyzer efficiency is based on HHV of hydrogen (El-Emam and Özcan 2019)

[c]Thermal energy can be produced from several energy sources: solar, geothermal, and nuclear

[d]The thermal efficiency is based on a higher heating value.

Table -4

FEEDSTOCK	ENERGY	PRODUCTION PROCESS	DESCRIPTION
Water	Solar	photolysis	Sunlight is used directly to produce H_2 from water. Long-term technology with low production efficiency.
	Electricity[a]	Electrolysis	Decomposition of water to H_2 and O_2 due to the electric. current passing through the electrolyzer. Commercial technology. H_2 production efficiency is 60–90%[b]
	Thermal[c]	Thermochemical water splitting (thermolysis)	Decomposition of water due to heat energy (~2500°C) Efficiency is about 50%
	Electricity[a] and solar	Photo-electrochemical water splitting	Water decomposition is due to sunlight and electricity Efficiency is about 12.4%
Biomass	Thermal	Gasification	Solid fuel reacts with O_2 and/or steam to produce H_2 and CO2 Efficiency is about 35–50% [d]
	Biochemical	Dark fermentation	Primarily anaerobic bacteria carry out the reaction,sometimes algae, that converts carbohydrate-rich matterinto H_2, CO_2, and other products Efficiency is about 60–80%
	Solar	Photo fermentation	Solar to hydrogen via organic materials occurs in light Efficiency is about 0.1%
	Electricity[a]	Microbial electrolysis cell	The use of electro hydrogenesis converts biodegradable material into hydrogen.

			Efficiency is about 78%
Hydrocarbons	Thermal[c]	Steam reforming	A steam reaction with liquid or gas fuel at a high temp pressure Efficiency is about 70–85%
		Partial oxidation	The reaction of hydrocarbons with O_2 at high tempera-tures The reaction of methane with O_2 Efficiency is about 60–75%
		Autothermal reforming	The reaction of O_2 and steam with hydrocarbons Efficiency is about 60–75%
		Thermal decomposition (pyrolysis	Hydrocarbons thermally break down into hydrogen and carbon when heated to a high temperature Efficiency is about 60%
		Steam–iron process	Steam–iron hydrogen synthesis is one of the earliest commercial processes. Coal is consumed cyclically by water cleavage. Coal is gasified to carbon monoxide and hydrogen.
	Electricity[a]	Plasma reforming	The same as the conventional reforming process Efficiency is about 9–85%
Other	Thermal[c]	Ammonia reforming	Use portable power applications Near-term technology
		Aqueous phase reforming	Use carbohydrates as a feedstock It occurs under 25–30 MPa and 220–270°C.

Table 4 Summary of the hydrogen production techniques according to feedstock types (Hacker et al. 2000; Steinfeld 2005; Kovács et al. 2006; Gupta 2009; Holladay et al. 2009; Zhang et al. 2016; Buttler and Spliethoff 2018; David et al. 2019; El-Emam and Özcan 2019 Hassan et al.

6.2. Alkaline Water Electrolyzer :

The AWE is an electrolyzer constituted by a diaphragm and two electrodes inside a liquid electrolyte water solution, which is in general almost 40% sodium hydroxide (NaOH) or potassium hydroxide (KOH). The diaphragm which separates the two electrodes in the solution allows the circulation of water molecules and hydroxide ions and separates the H_2 and O_2 for safety and purity aspects. The purity of the hydrogen produced is 99.5 to 99.9%, and it can reach 99.99% by using catalytic gas purification processes. The performance of this kind of electrolysis is affected by the diaphragm, anode, and cathode material type and thickness. The AWE and the PEM use two different types of electrolytes: the PEM uses a solid polymer membrane electrolyte, but the AWE uses a corrosive liquid electrolyte.

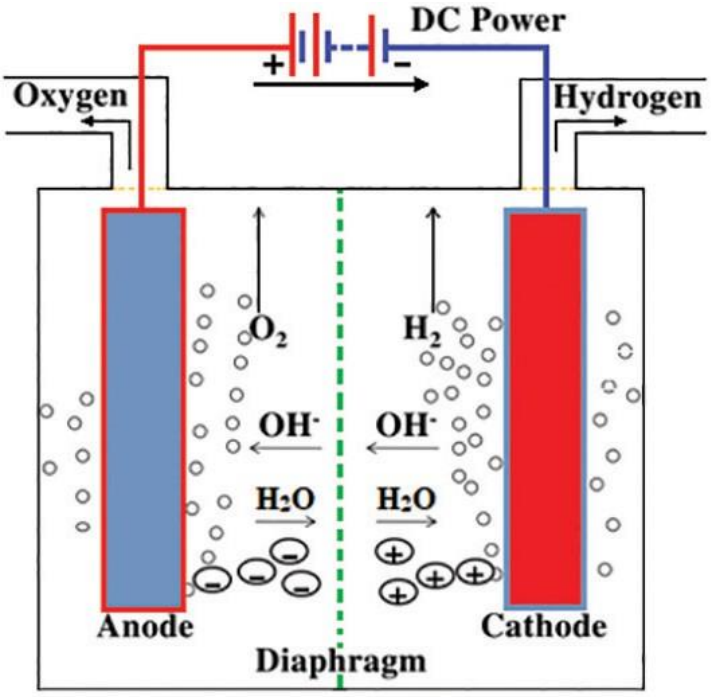
The conductivity of the solution is enhanced by the use of strong electrolytes that deliver ions with high mobility [43], such as sodium, potassium for positive ions, and hydroxide or chlorides as negative ions. During electrolysis, the water molecules move to the cathode by diffusion as they are consumed, and the hydroxide ions move to the anode by migration because they have an opposite charge and diffusion because they are consumed. A diaphragm separates the two anode and cathode compartments and the gases formed are thus collected: hydrogen at the cathode and oxygen at the anode as shown in Figure.

Concentrated solutions of potassium hydroxide are generally used as the electrolytic solution because they have very high conductivities and fewer corrosion problems compared with other alkaline electrolytes. The electrode materials often used are based on nickel because of its low cost, high activity [52].

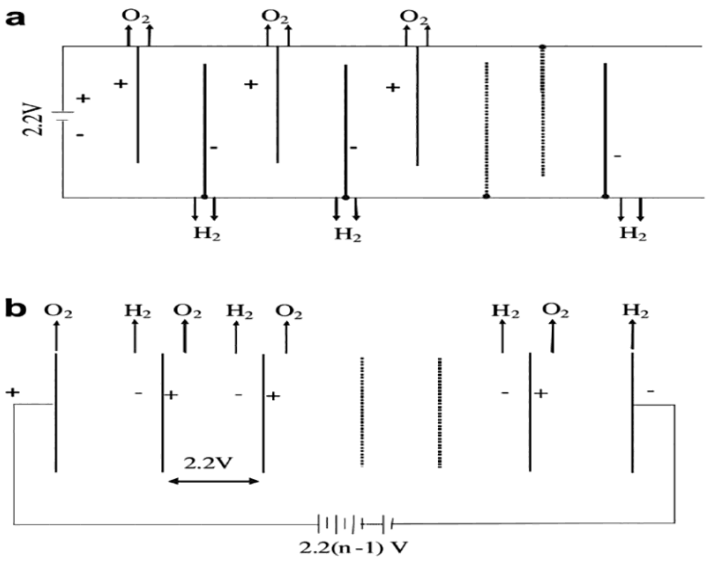
Electrolysis cells can be of two types of configurations: monopolar and bipolar [14]. Figure 4(a) gives a schematic of the monopolar configuration. The electrodes are altered in the electrolyzer and are all directly connected to the terminals of the DC power supply: the anodes at the positive terminal and the cathodes at the negative terminal. The total voltage applied to the entire electrolysis cell is essentially the same as that applied to the individual pairs of theelectrodes in the cell ($U_{tot} = U_i$), but the current is subdivided between the different unit cells ($I_{tot} = n \times I_i$). Figure 4(b) depicts conflation in bipolar mode. Only the two end electrodes are connected directly to the DC power source. The other inner electrodes have a dual role: one side acts as the cathode for a unit cell and the other side acts as the anode for the adjacent unit cell. These cells are electrically linked thanks to their electrodes which are bipolar and ionically via the electrolytic solution. The total voltage of the cell is the

sum of the individual voltages of the unit cells ($U_{tot} = n \times U_i$), but the current for each unit cell is equal to the output current of the generator ($I_{tot} = I_i$). The electrical energy consumed is the same in the two configurations.

The wide range of flammability limits of the mixture of hydrogen and oxygen requires a careful design of the electrolyzer system. The separator diaphragm (or membrane) must avoid the mixing of the two gases inside the cell. Furthermore, the corrosive nature of the electrolyte does not allow leaks that are often likely to take place at the connections and seals of the electrolyzer. The bipolar configuration is more risky in mixing oxygen and hydrogen because of their simultaneous productions on the same bipolar electrode (on each side) and also electrolyte leakage as the monopolar design.[47]



Obviously, the life of the system is an important criterion. It is extremely linked to the quality of the materials used. Indeed, these materials must be resistant to high concentrations of the alkaline electrolyte and operating conditions of the electrolyzer (pressure and temperature). In particular, connections and seals are subject to corrosion, which is why it is recommended to use sealing materials that are also stable in this environment [52].



6.3. Alkaline Anion Exchange Membrane:

The AEM is considered to be a combination of the PEM and the AWE. The advantages of the PEM and the AWE are merged in the AEM. So, the AEM uses a low-concentration alkaline solution as opposed to a 20–40% KOH or NaOH aqueous solution with a solid electrolyte (polymeric) membrane. The anode in an AEM is composed of Ni-based or titanium materials, and the cathode includes Ni, Ni-Fe, and $NiFe2O_4$. The AEM, short for Anion Exchange Membrane, stands out as a remarkable technological advancement within the field of electrochemistry. It is recognized as a unique integration of the Proton Exchange Membrane (PEM) and the Anion Exchange Membrane (AWE), effectively consolidating the benefits offered by both systems. Unlike traditional setups that rely on a relatively high concentration of either potassium hydroxide (KOH) or sodium hydroxide (NaOH) in aqueous solutions along with solid polymeric electrolytes, the AEM takes a different approach by utilizing a low-concentration alkaline solution. This innovative design not only enhances the efficiency but also offers a more sustainable and cost-effective solution. Moreover, the utilization of specific materials such as nickel-based alloys or titanium for the anode and varying compositions including nickel, nickel-iron, and nickel ferrite for the cathode further highlights the versatility and adaptability of the AEM technology.

6.4. High-Temperature Steam Electrolyzer :

The HTSE, also known as a high-temperature steam electrolyzer, functions by utilizing steam at elevated temperatures. One of the primary advantages of this advanced technology lies in

its efficient utilization of steam compared to liquid water, resulting in reduced energy requirements. Unlike conventional methods, the HTSE efficiently breaks down water molecules using heat rather than electricity. By leveraging this thermal approach, the process significantly enhances efficiency levels while concurrently driving down the overall production costs associated with hydrogen generation. This innovative method not only streamlines the decomposition of steam but also contributes to a more sustainable and cost-effective hydrogen production process in the long run.

6.5. Solid Oxide Electrolyzer:

Solid oxide fuel cells (SOFCs) are indeed versatile devices that can operate in both fuel cell and electrolysis modes. In the electrolysis mode, they can convert water vapor into hydrogen gas and oxygen. One of the key advantages of using SOFCs for electrolysis, particularly at high temperatures, is the significant reduction in electrical consumption and the associated cost savings. Here are some key points based on the information you provided:

- High-Temperature Operation: Operating the electrolyzer at high temperatures offers several advantages. First, the increased temperature provides additional energy input in the form of heat, which supplements the electrical energy input. This heat input is often more economical compared to using purely electrical energy. Additionally, higher temperatures enhance the overall efficiency of the electrolysis process.
- Energy Efficiency: The high-temperature operation and the use of oxygen ion conducting ceramics as the electrolyte contribute to the high efficiency of SOFC-based electrolyzers. These ceramics, such as ZrO2 stabilized by Y2O3, MgO, or CaO, allow for efficient transport of oxygen ions, which is crucial for the electrolysis process.
- Improved Kinetics and Reduced Energy Loss: The elevated temperature promotes better conduction of the electrolyte and accelerates the kinetics of the electrochemical reactions involved. This leads to reduced energy losses due to electrode polarization, further enhancing the overall efficiency of the electrolyzer.
- Operational Parameters: Typically, high-temperature SOFC electrolyzers operate in the temperature range of 800–1000°C. Water vapor is introduced into the cathode, where it is converted into hydrogen gas and oxygen ions. The oxygen ions then travel through the solid electrolyte to the anode, where they participate in oxidation reactions to produce gaseous oxygen.

- Efficiency Comparison: High-temperature electrolyzers based on SOFC technology can achieve impressive electrical efficiencies, often around 92%. In contrast, electrolyzers operating at lower temperatures typically max out at around 85% efficiency.

Overall, the use of high-temperature SOFCs for electrolysis offers a compelling combination of energy efficiency, cost-effectiveness, and improved reaction kinetics, making them a promising technology for hydrogen production and other applications.

Table -5

Specification	**PEM**	**AEM**	**AWE**	**SOE**
Maturity	Commercial	Commercial	Commercial	Early Commercial
Charger carrier	H^+	OH^-	OH^-	O^{2-}
Electrolyte	Solid polymer	Solid polymer	Aqueous solution10-40% KOH/NaOH	Solid ceramic
Working fluid	Distilled water	Distilled water or Low concentration solution	High concentration solution	Steam
Anode material	Pt; Ir; Ru	Ni-based alloy	Ni	LSMYSZ; $CaTiO_3$
Cathode material	Pt; Pt=C	Ni, Ni-Fe, $NiFe_2O_4$	Ni alloys	Nicermets
Temperature,	70-90	50-70	65-100	650-1000
Operation pressure.	15-30 bar	up to 35 bar	2-10 bar	<30 bar
Efficiency, HHV	67-84%	-	62-82%	~90%
Cell voltage	1.80 2.40 V	~ 1.85 V	1.80 2.40 V	0.95 1.30 V
Current density	0.6-2 A/cm^2	0.1-0.5 A/cm^2	0.2 0.4 A/cm^2	0.3 1 A/cm^2
Startup duration	<15 minutes	-	15 minutes	>60 minutes
Stack lifetime	< 40,000 hr	> 10,000 hr	< 90,000 hr	< 40,000 hr

Energy consumption, kWh/Nm^3	4.5-7.5	~ 4.8	4.5-7	2.5-3.5
Estimated cost by 2050.	$750/kWch	-	$600/kWch	$200/kWch
Advantages	Compact and simple design. Fast response andstartup. High hydrogen purity.	A mixture of the advantages of PEMand AWE. Suitable for load fluctuation. Cheap components.	Low capital cost. Stable and well-established. No use of noble material.	It can be used as afuel cell. High efficiency. Due to the absenceof noble material, the capital cost is low.

Comparison between different types of water electrolyzers (Dincer and Acar 2014; Chi and Yu 2018; El-Emam and Özcan 2019; Hosseini and Wahid 2020; Burton et al. 2021; Motealleh et al. 2021; Li and Baek 2021).

7. Challenges of water electrolysis

the challenges facing water electrolysis for hydrogen generation are multifaceted. While there's a push to commercialize this technology and reduce both investment and operational costs, significant hurdles remain.

- Costs: As you mentioned, the costs associated with electrolysis systems are high. This is primarily due to the materials used in the electrolyzers, such as precious metals like platinum and iridium, which contribute to the overall expense.
- Intermittent Energy Sources: Renewable energy sources like solar and wind are intermittent by nature, meaning they don't produce a consistent output. This intermittency can affect the efficiency and reliability of electrolysis systems, as they rely on a stable and continuous energy supply.

- Water Consumption: Water is a crucial resource, and large-scale electrolysis operations can consume significant amounts of it. This raises concerns about the environmental impact, especially in regions where water scarcity is already an issue.
- Efficiency: Improving the efficiency of electrolysis systems is another key challenge. Higher efficiency means less energy input required to produce a certain amount of hydrogen, ultimately reducing costs and resource consumption.

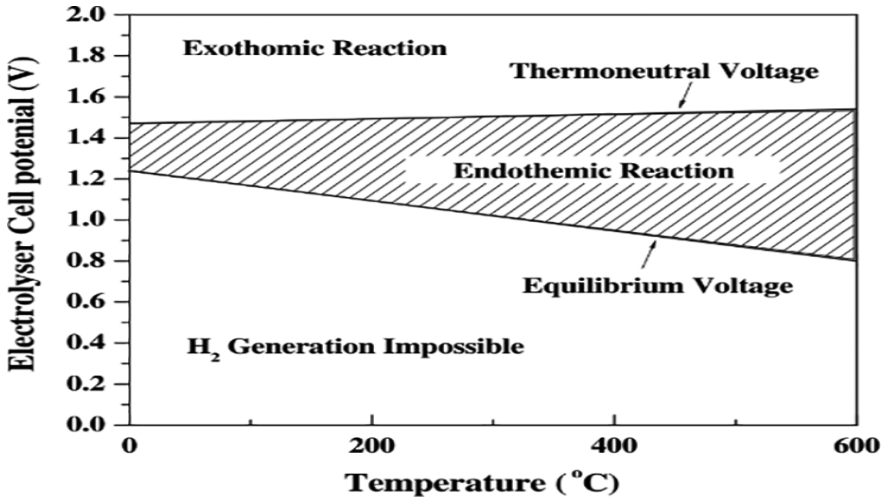
these challenges requires a multi-faceted approach involving advancements in technology, materials science, renewable energy infrastructure, and water management practices. Collaborative efforts between industry, academia, and government agencies are crucial to overcoming these obstacles and making water electrolysis a more attractive and sustainable method for hydrogen production(Younas et al. 2022).

8. Cell voltage (difference of potential)

The potential difference for a cell of an electrolyzer, which is always ΔE = 1:8˜2:0 V at the current density of j = 1000 ˜ 300 Am2 in industry water electrolysis [17], is an addition of four terms:

$$\Delta E = \Delta E_{the} + \eta_a + \eta_c + R.I \qquad 11$$

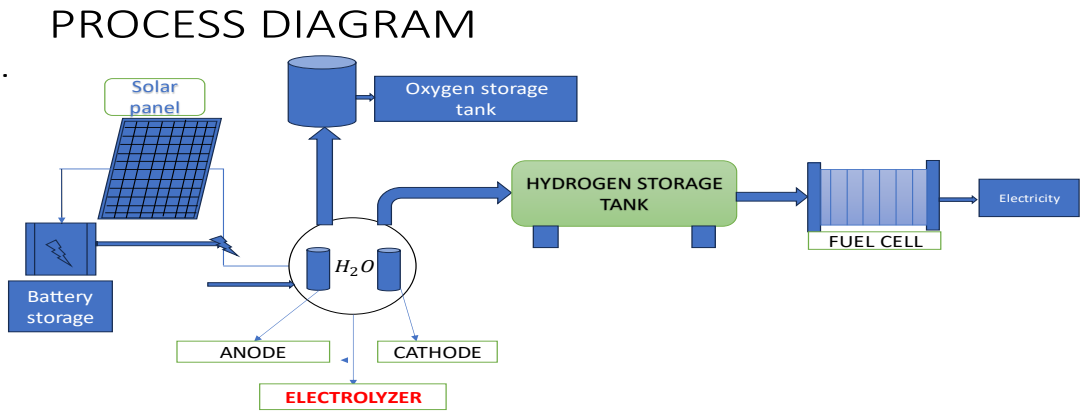
with: ηa(V) is the anodic overvoltage; ηc(V) is the cathodic overvoltage; R (Ω) is the global resistance and I (A) is the current. Figure shows the relationship between the electrolyzer cell potential and operating temperature [51,52,53]. The cell potential-temperature plane is divided into three zones by the so-called equilibrium voltage line and thermo-neutral voltage line. The equilibrium voltage is the theoretical minimum potential required to dissociate water by electrolysis, below which the electrolysis of water cannot proceed. The equilibrium voltage decreases with increasing temperature. The thermo-neutral voltage is the actual minimum voltage that has to be applied to the electrolysis cell, below which the electrolysis is endothermic and above which, exothermic. The thermoneutral voltage naturally includes the overpotentials of the electrodes, which are only weakly dependent on temperature.



9. Green electricity production systems

Solar strength produces sufcient energy to pressure electrolyzers for hydrogen storage or direct use at some point of manufacturing. Normal examples of solar strength are photovoltaic (PV) and focused sun electricity (CSP) structures (Soliman et al. 2019). But, wind turbines used to convert solar to energy are an example of sun electricity. Even though PV panels are without delay coupled with electrolyzers, CSP is frst related to a energy cycle for energy production earlier than connecting them to electrolyzers. Therefore, the want for an AC/DC or DC/DC converter is mandatory in electrolyzer load adjustments.Green production gives a great method to provide far off areas with electricity because of the high price of power transmission (Singla et al. 2021). Therefore, excess energy from renewable resources has been used to operate electrolyzers for hydrogen manufacturing. Hydrogen also can be used in gas cells to provide power throughout the night or intermittency. Affords the simple concept of a sun hydrogen manufacturing system.

In a PV/hydrogen production (PV/H2) scheme, PV panels are connected to an electrolyzer via a capacity-adapting part holding a maximum strength point following (MPPT) gadget and a DC/DC preacher. This part is exploited to blow up the harvest from panels and regulate the electrolyzer input strength (Haider et.al 2021; Nasser et.al 2022b). However, in the case of extravagance energetic strength from PV systems, a assault structure is selected as capacity depository. Therefore, the principal benefts of the PV/H2 novelty over other constructions are the use of a DC energetic strength product and the lack of switching parts,which leads to minor support.



The schematic diagram for solar hydrogen production systems

Contrastively, in the CSP/hydrogen result (CSP/H2) plan, energy from the sun heat is detached into two portions: the frst is used in capacity phases (for instance, unaffected Rankine phase (ORC)) to produce electricity that drives the electrolyzer, and the second converts water to energy by way of utilizing SOE, as subpoenaed in Fig.(Chadegani et.al 2018). Based on this principle, the system may have thermal storage to ensure continuous production at night. A previous study compared PV/H2 and CSP/H2 under the same conditions to investigate their system performances (Joshi et al. 2011). The results revealed that the CSP/H2 system performed better than PV/H. Comparatively, the hydrogen production system is more like a PV/H2 system but needs an AC/DC converter to drive the electrolyzer. illustrates the essential components of this system. Interestingly, a combination of these energy sources can be applied to enhance a system's effciency and provide a multi-generation cycle. Therefore, this possibility is discussed in detail in the current study.

10. PV/H2 case studies

Several case studies have happened administered to estimate and resolve hydrogen result amounts, containing the cost of bearing 1 kg of hydrogen utilizing PV panels under different of or in the atmosphere environments (for instance, Algeria and Morocco). For example, a mathematical study was transported in the United States to show the strength of the PV/H2 structure to supply the frst two fuel container buses accompanying hydrogen (Vidueira et.al 2003). Their searches disclosed that bureaucracy keep specify the buses accompanying enough hydrogen to work all era outside issuance. In added studies, while the potential for

hydrogen result in in the south Algerian domains confirmed better than in the northerly regions by 45% under the unchanging environments (Mokhtara et.al2020; Khelfaoui et.al 2020), different domains of Algeria written a greater hydrogen supporting duction than North African nations (Saadi et.al2016). For instance, under the Moroccan environment, LCOH categorized from 4.64 to 5.79 $/kg when the power cost from PV panels was 0.077–0.099 $/kWh (Touili and others. 2018). Hence, a study distinguished fxed PV, PV accompanying a radio detecting and ranging, and a Stirling food for H2 result in few domains (Touili et.al 2020). LCOH Several case studies have happened administered to estimate and resolve hydrogen result amounts, containing the cost of bearing 1 kg of hydrogen utilizing PV panels underdif ferent of or in the atmosphere environments (for instance, Algeria and Morocco). For example, a mathematical study was transported in the United States to show the strength of the PV/H2 structure to supply the frst two fuel container buses accompanying hydrogen (Vidueiret.al 2003). Their searches disclosed that bureaucracy keep specify the buses accompanying enough hydrogen to work all era outside issuance. In added studies, while the potential for hydrogen result in in the south Algerian domains confirmed better than in the northerly regions by 45% under the unchanging environments (Mokhtara et.al2020; Khelfaoui et.al2020), different domains of Algeria written a greater hydrogen supporting duction than North African nations (Saadi et.al 2016). For instance, under the Moroccan environment, LCOH categorized from 4.64 to 5.79 $/kg when the power cost from PV panels was 0.077–0.099 $/kWh (Touili et.al 2018). Hence, a study distinguished fxed PV, PV accompanying a radio detecting and ranging, and a Stirling food for H2 result in few domains (Touili et.al 2020).

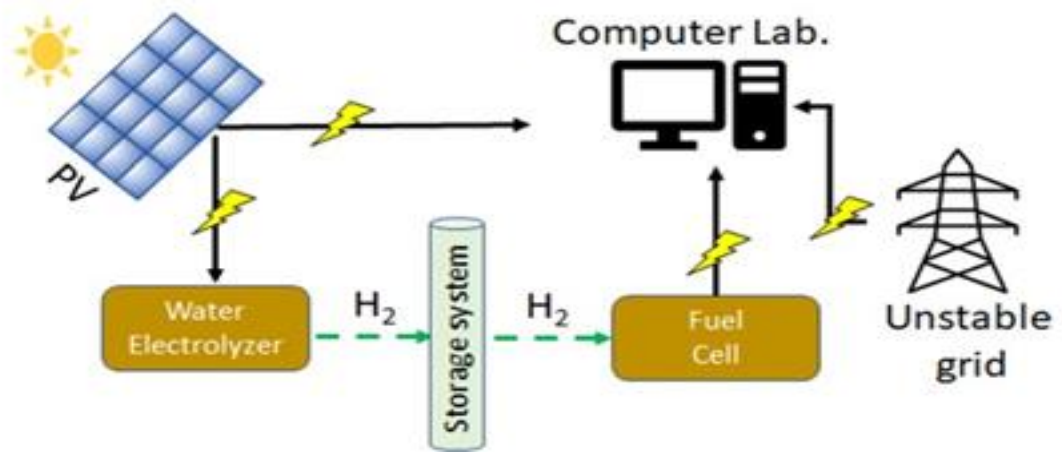
11. PV/H2 system

The PV/H2 method is a hopeful technique for green hydro gen result on account of allure economically competitive, com mercially practicable, and tenable structure (Bhattacharyya and others. 2017). Therefore, this arrangement has existed investigated under different important environments accompanying and without a cosmic radio detecting and ranging (Bilgen 2001).Notably, a study indicated that even though bureaucracy accompanying solar following had greater conduct, its capital cost was bred. Moreover, utilizing concentrated PV raised bureaucracy efciency from 12 to 16% as well the non-concentrated individual (Bicer and Dincer 2017). Hence, the analytical study had the alike results as the experiment (Ismail et al. 2019).

This study investigated the system's performance with and without MPPT (Ganeshan et al. 2016). Their investigations revealed that although the system with direct coupling had an efciency close to the system with MPPT, the capital cost of the system with MPPT was higher. Another study also mentioned that increasing MPPT effciency increased hydrogen production (Rahim et al. 2015). Therefore, the PEM electrolyzer is suitable for PV/H2 due to its ability to deal with load fuctuation and its lowest cold startup property, among other types (Paul and Andrews et.al2008), as illustrated. electric load consumption (Richards and Conibeer 2007). Investigations revealed that this system was more suitable as a stand-alone system in arid areas and areas with high elevations (Valdés et al. 2012). It was also reported that the tilted PV panels possessed higher effciency during hydrogen production in a stand-alone system than horizontal panels (Tebibel et.al2017). However, the PV/ H2 system without a battery requires fewer PV panels and involves low LCOH. Therefore, coupling PV panels with a water electrolyzer to produce the necessary hydrogen for fuel cells and provide electricity during the night or winter is a promising technique for the future (Lagorse et al. 2008). Alternatively, buying power to perform the electrolyzer during energy from the sun of-periods is economically practicable on account of the increase in occupied hours (Ferrari et.al 2016). The results illustrated that since the LCOH principles for gridiron/H2, gridiron +PV/H2 , and PV/H2 were 5.5, 6.1, and 12.1 $/kg, individually (Shaner 2016; Grimm et al. 2020; Matute et.al 2022), the system's cost maybe renewed in 12 age. They likewise found that the enormous capital cost was principally on account of land costs and the amount secondhand for PV committee explanation. Therefore, detached areas accompanying plentiful energy from the sun are thought-out more acceptable locations for this type of plant. Since the optimum unification middle from two points PV panels and water electrolyzers is necessary to specify extreme hydrogen production by growing a system's efciency, monofacial and bifacial PV panels are secondhand in PV/H2 schemes to show their affect efciency under akin operating conditions (Privitera and others. 2020). Investigations told that the efciency be honest to 13.5% for bifacial PV panels alternatively 11.55% for monofacial PV panels. Based on the bifacial PV, they likewise noticed that hydrogen production raised from 3.7 to 4.2 g/h per square rhythm.

Remarkably, it was currently noticed that an ultrahigh aggregation PV/H2 scheme manage better a method's ef ciency to nearly 18–21% alternatively 9.4% for unoriginal PV, accompanying allure hydrogen result grazing from 0.8 to 1.0 L/brief time period per square beat for reduced PV/H2 (Muhammad-Bashir et.al 2020). Although the assault increases

bureaucracy capital cost, it reduces the electrolyzer's proportion and allows hydrogen result each evening, including an LCOH about 6–7 €/kg (Gutiérrez-Martín et.al 2020; Zhang and Wei 2020; Puranen et.al 2021). Likewise, DCX converters use a extreme-efciency DC service in PV/H2 to increase bureaucracy's efciency (Concha et.al 2021). Since the depiction of normal PV panels increases by lowering their hotness, photovoltaic ther mal (PVT) can present extreme-power gain plus heat strength for various purposes (Li et.al 2022) (Soliman and Hassan et.al 2019).



PV/H_2 system provides enoughelectricity to computer lab because of unstable electric supply from the grid [Okundamiya et.al 2020]

As a result, this power increases the hydrogen result from an electrolyzer, with lowering result costs. Furthermore, while air, water, and nanofuids as chilling fuids can decrease the PVT hotness, crop fuid from PVT maybe secondhand for warming (Gado et.al 2022). Consequently, hydrogen result from pairing PV, PVT/air, and PVT/water accompanying water electrolyzer reaches until 8.19, 13.9, and 17.12 mL/brief time period, individually (Senthilraja and others. 2020), inasmuch as PVT/nanofuids increase the capacity gain by 47% distinguished accompanying PVT/water (Sangeetha et.al 2021).

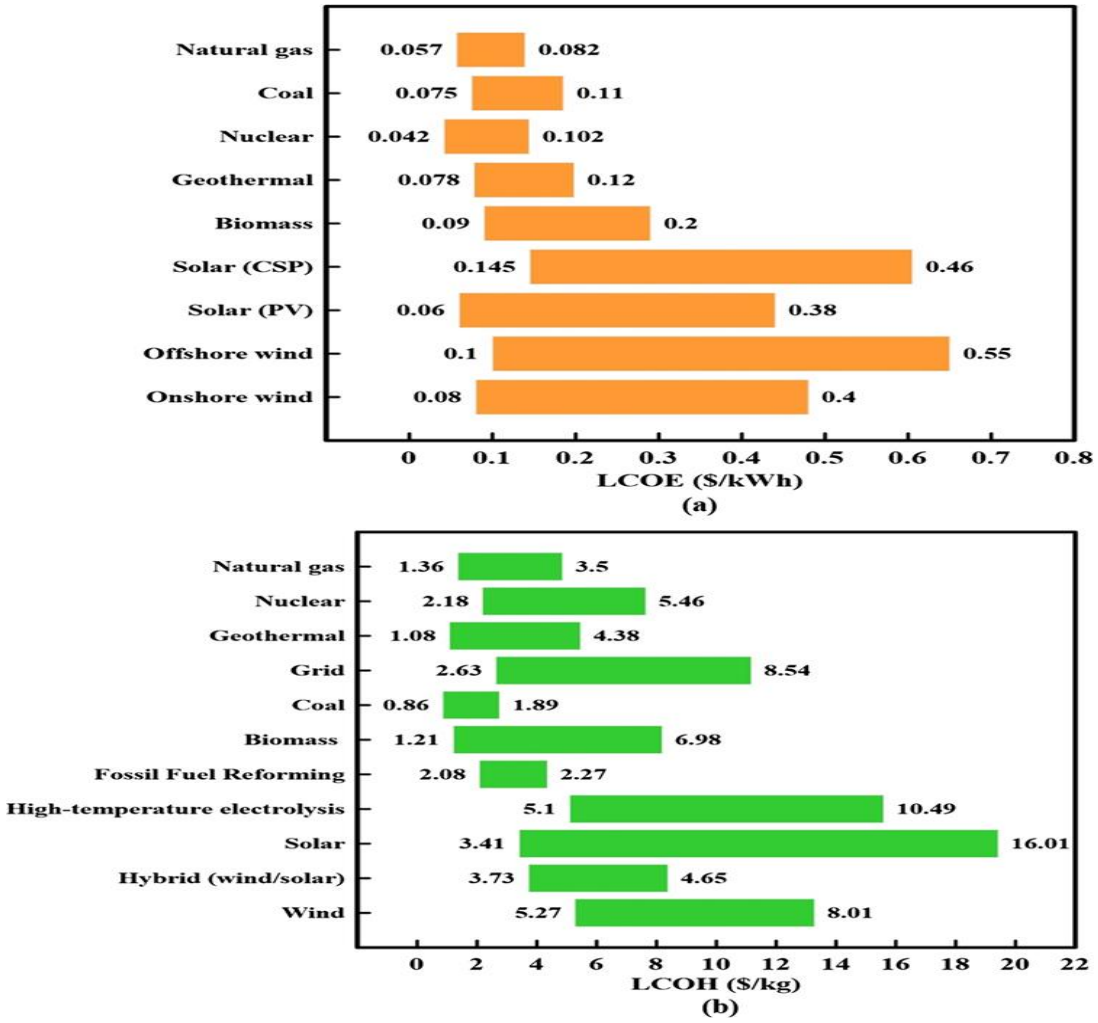
Therefore, these methods are now enticing more consideration on account of their souped up distinguished to usual PV/H2 arrangements. encapsulates the multi-era methods and their main specifcations. Consequently, while the PV and PVT panels specify heat and power demand for constructions (Elghamry et.al 2019), their extravagance power drives the electrolyzer for hydrogen. Hydrogen especially drives fuel containers to specify heat, power, and occasionally drink water. Hence, in essence, utilizing the Hofmann voltammeter

electrolyzer allows investigators to act pretreatment for wastewater to humble contaminants. Besides hydrogen result, bureaucracy maybe secondhand for liquid result (Siddiqui and Dincer et.al 2020). The results told that bureaucracy exergy efciency reaches until 55.5% and the caused liquid is until 1949.8 kmol, while hydrogen result is until 5849.3 kmol.

12. Economic assessment of green hydrogen production

Electricity plays a essential function in hydrogen result cause it is the basic recommendation to electrolyzers that controls hydrogen result costs. Moreover, various determinants in the way that the period, land cost, and construc- tion ending influence power result's reducing from energy from undepletable source. Fig bellow explains the LCOE(the analysis of capital and operating cost in the hydrogen production process) associations for various strength beginnings (inexhaustible and nonrenewable) (Shen and others. 2020). This figure shows that even though usual capacity beginnings like bitumen and basic have hostile LCOE, they otherwise influence the envi ronment on account of green vapor diffusions. In contrast, while energy from undepletable source beginnings have greater LCOEs than tra ditional one, they are chosen existing cause the experience is difficult to convert to nothing diffusion capacity type tion, suggesting that allure cost will be deprived of When calculating LCOH, electricity cost directly affects the results (Nasser et al.2022b). Fig. illustrates the LCOH for different techniques (El-Emam and Özcan 2019; Razi and Dincer et.al 2020).

As shown in this figure, the production methods that depend on conventional energy sources had lower LCOH than green methods. Notably, although these methods were expensive, they have attracted more attention for being used in constructing a sustainable society. For example, while the LCOH produced from solar and wind energies varied from 3.41 to 16.01 $/kg and 5.27 to 8.01 $/kg, respectively, the LCOH of a hybrid system lay in the midway of the solar.



The range of (**a**) LCOE and (**b**) LCOH from different energy sources (El-Emam and Özcan 2019; IEA 2020; Razi and Dincer et.al 2020; Shen et al. 2020; Wu et al. 2021.

Climatic conditions also play a crucial role in producing electricity and hydrogen from solar and wind energy due to the dependence of these sources on climate. As a result, the production of each system mentioned in this study is influenced by location changes from one place to another. Fig. illustrates the LCOH gathered from this review for the understudied systems. This figure demonstrates that although the LCOH varied by the country for similar designs, the average cost of hydrogen production for solar because it worked day and night.

Studies have also reported that the electrolyzer type cou- pled with similar energy sources changes the LCOH. For example, LCOH from wind energy associated with PEM varies from 5 to 9.37 $/kg (Olateju et al. 2014, 2016; El- Emam and Özcan 2019). However, for AWE, the LCOH ranged from 7.47 to 7.6 $/kg (Greiner et al. 2007). In other studies, the LCOH when SOE is used varies from 6 to 9.2$/kg and should decline to 2 $/kg by 2050

(Mastropasqua et al. 2020; Khatiwada et al. 2022). Thus, to sum up, the two main parameters that influence the LCOH from renewable sources are (I) weather conditions (e.g., solar radiation and wind speed) and (II) electrolyzer type.

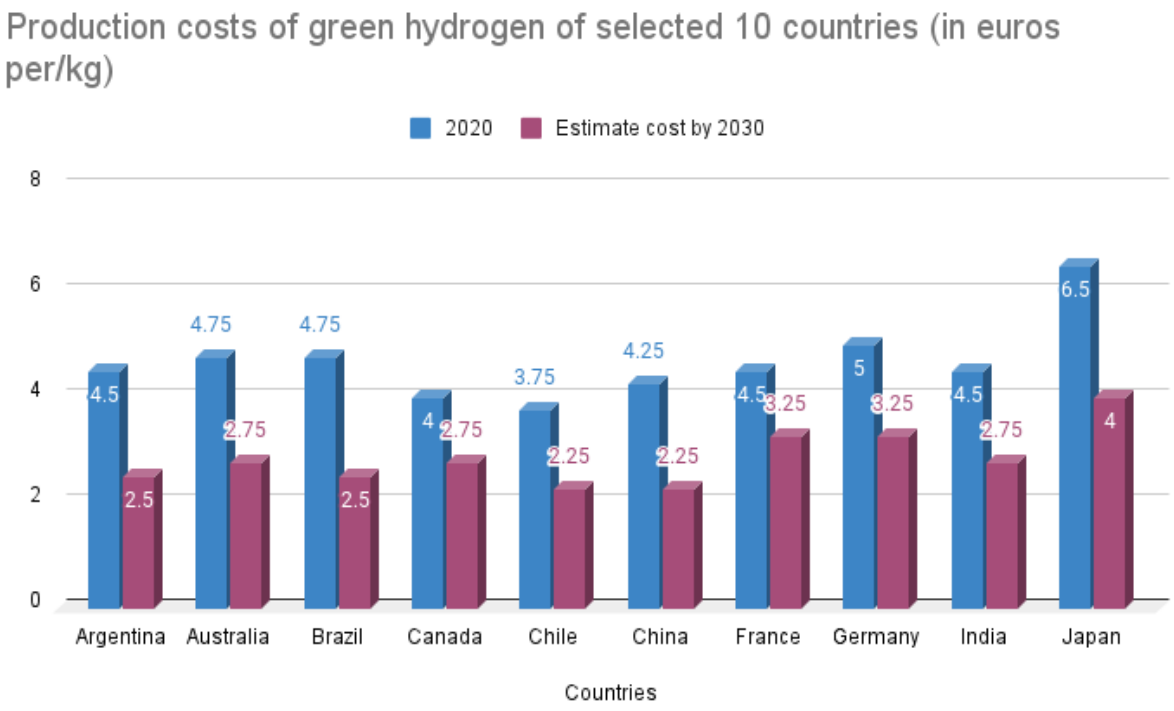


Fig. according to the country of production (data collected from the review)

13. Economic challenges

The production of green hydrogen is currently experiencing high costs, primarily due to a lack of external support and operational challenges. This issue is particularly prevalent in underdeveloped regions that have abundant water resources suitable for hydrogen production. Despite the underestimated costs associated with green hydrogen, there is a noticeable hesitation and limited demand for its adoption. Even in areas with ample renewable energy sources, such as solar and wind power, the expenses linked to power consumption play a significant role in the overall production costs of green hydrogen. In order to address this challenge, industry experts are advocating for an enhancement of their energy budgets to facilitate the widespread adoption and production of green hydrogen. One potential solution could involve utilizing revenues generated from the reduction of hydrocarbon reserves to finance green hydrogen initiatives. However, scaling up production would require the establishment of a robust hydrogen infrastructure, necessitating extensive planning and

governmental backing. To navigate this complex landscape, experts may consider forming partnerships with established companies to collaboratively develop a strategic roadmap for advancing the use of green hydrogen within various industries and shaping the future landscape of sustainable energy production (Agaton et.al 2022).

14. Ways of storing renewable hydrogen

Hydrogen has the potential to address two major challenges in the global drive to achieve net zero emissions by 2050. First, it can help tackle the perennial issue of the intermittency of renewable energy sources such as wind and solar. By converting excess power generated on windy or sunny days into hydrogen, the gas can store renewable energy that can then be dispatched at times of peak demand as a clean fuel source for power generation. Second, hydrogen can replace fossil fuels to decarbonize sectors where electrification alone won't suffice, such as domestic heating, industry, shipping and aviation. The hitch is that, while an excellent medium for renewable energy storage, hydrogen itself is hard to store.

This is because it has a low volumetric energy density compared to other gases — such as natural gas meaning it takes up significantly more space. Also, hydrogen has a boiling point close to absolute zero and requires cryogenic storage. And while it does not typically corrode storage containers, it can cause cracks in metals under certain conditions.

14.1. Geological hydrogen storage

One of the most significant developments in renewable energy infrastructure is taking place in Utah, United States, where the Advanced Clean Energy Storage Hub is currently being constructed. This hub, once completed, will serve as a pioneering showcase of cutting-edge technologies geared towards facilitating a transition to a decarbonized power grid of the future. Central to this ambitious project is the integration of green hydrogen production, storage, and distribution in a comprehensive system that promises to revolutionize the way we harness and utilize renewable energy sources.

Playing a crucial role in this groundbreaking initiative is Mitsubishi Power, a distinguished power solutions brand under the umbrella of Mitsubishi Heavy Industries (MHI). Leveraging its expertise and innovative solutions, Mitsubishi Power is spearheading the development of the hydrogen production technology that will enable the conversion of renewable energy sources into hydrogen fuel. The captured hydrogen will then be stored in a network of salt caverns that are strategically located deep underground within a vast salt dome covering an extensive area of over 4,800 acres. These caverns, each measuring approximately 67 meters

in diameter and towering at a height of 580 meters, will provide a robust storage solution for the generated green hydrogen, ensuring its availability for future energy needs. Mitsubishi Power's involvement in a parallel venture with Texas Brine in the United States underscores the company's commitment to advancing sustainable energy solutions. In this collaborative endeavor, extensive efforts are being made to extract salt from enormous underground caverns, thereby creating ample space for the storage of hydrogen. By capitalizing on the proven efficacy of gas storage in salt caverns, Mitsubishi Power is paving the way for seamless knowledge transfer and operational success within the realm of renewable energy storage. Additionally, these salt caverns, alongside other geological structures such as depleted oil fields and aquifers, further broaden the spectrum of viable options for geological storage, reinforcing the versatility and resilience of energy storage solutions in a rapidly evolving landscape.

14.2. Liquified hydrogen storage

Liquid hydrogen, while highly efficient as a storage method, poses significant technical challenges due to its requirement of extreme cryogenic temperatures. To elaborate, the process involves cooling the hydrogen gas to a bone-chilling -253°C, a temperature at which it transitions into a liquid state. This transition is crucial for maintaining its stability and significantly reducing evaporation rates, ensuring that the hydrogen remains in a usable form. The storage of liquid hydrogen necessitates specialized insulated tanks that are capable of sustaining such low temperatures. Consequently, the infrastructure for liquid hydrogen storage involves intricate engineering and extensive safety measures to prevent any potential hazards associated with its unique properties. the unparalleled efficiency of liquid hydrogen as a storage medium, the complexity involved in its storage and the exhaustive maintenance required have traditionally rendered it a costly option. The infrastructure needed to support liquid hydrogen storage is intricate and demands meticulous attention to detail to ensure safety and operational efficiency. Moreover, the cooling and maintenance of hydrogen at cryogenic temperatures necessitate the use of advanced technology and sophisticated engineering processes, further adding to the cost implications. This technical complexity has been a deterrent to wider adoption and utilization of liquid hydrogen as a mainstream storage solution across various industries.

Despite these challenges, the use of liquid hydrogen for specialized applications, such as rocket fuel in the aerospace industry and for semiconductor manufacturing, has demonstrated its efficacy and benefits. The controlled handling and storage of liquid hydrogen are essential

in these high-demand sectors, where precision and reliability are paramount. However, the broader adoption of liquid hydrogen storage technologies has been limited by the associated costs and technological barriers. The current landscape of hydrogen storage technologies is evolving, driven by the rising demand for sustainable energy solutions and the need to enhance energy storage capacities. As the industry transitions towards a more hydrogen-centric future, advancements in liquefaction technologies are paramount to achieving scalability and cost-effectiveness. The recent milestone of the first shipment of liquefied hydrogen between Australia and Japan signifies a pivotal moment in the global hydrogen market, highlighting the importance of scaling up critical technologies like liquefaction. This development underscores the potential for greater economies of scale in liquid hydrogen storage and transportation, paving the way for a more efficient and sustainable energy storage solution.

In conclusion, while liquid hydrogen storage presents unique challenges in terms of complexity and cost, ongoing advancements in technology and infrastructure are driving the industry towards a future where liquefaction becomes a more accessible and economically viable option for storing and transporting hydrogen.

14.3. Compressed hydrogen storage

Like any gas, hydrogen can also be compressed and stored in tanks, and then used as needed. However, the volume of hydrogen is much larger than that of other hydrocarbons nearly four times as much as natural gas. For practical handling purposes, hydrogen therefore needs to be compressed. For example, fuel-cell powered cars run on compressed hydrogen contained in large, highly pressurized containers.If an application requires hydrogen volume to be reduced further than compression can achieve, it can be liquefied. The two techniques compression and liquefaction can also be combined.Hydrogen’s low energy density, high volume and need for cryogenic storage are some of the biggest barriers to its growth. This is especially true for mobility applications such as heavy transport, where the space and other requirements for hydrogen storage would drastically reduce the room for passengers and cargo. The same applies to vehicles, where a balance needs to be struck between passenger space and range.

One solution is a new type of tank for the automotive sectorone of many hydrogen infrastructure projects supported by the European Union.

14.4. Materials-based storage

An opportunity to compressed and liquefied hydrogen is materials-primarily based totally storage. Here, solids and beverages which can be chemically capable of take in or react with hydrogen are used to bind it. This consists of growing metallic hydrides from factors inclusive of palladium that may take in 900 instances its personal quantity in hydrogen — in addition to magnesium, aluminum and positive alloys.Using ammonia — a compound of hydrogen and nitrogen — as a provider for hydrogen is, arguably, the choice with the maximum potential. Its strength density via way of means of quantity is almost double that of liquefied hydrogen, making it a long way simpler to keep and transport.

This way that hydrogen is transformed to ammonia, transported to its vacation spot and then “cracked” to launch the hydrogen at its factor of use. Ammonia cracking continues to be withinside the early improvement degree and conversion fees stay low — round a 3rd at best. It has been cautioned that ammonia may want to turn out to be the “workhorse” of a destiny hydrogen society, specially wherein direct use of hydrogen isn't always an option. Countries inclusive of Japan and South Korea are seeking to import ammonia as they've much less possibility to provide hydrogen and get it to direct offtakers. For example, MHI`s shipbuilding department is designing a vessel so as to be powered via way of means of and additionally deliver ammonia.

Most nations in Europe and the United States are much more likely to prioritize hydrogen as it could be extra without difficulty produced and ate up locally, inclusive of inside business clusters or thru pipelines. extra than one hundred low-carbon hydrogen initiatives indexed in Wood Mackenzie`s Hydrogen Project Tracker, over 85% combine ammonia and hydrogen to serve home and export markets.

15. Future prospects

- Green synthesis of NiO nanoparticles using plant extract or other biological materials is deemed as a highly appropriate and eco-friendly method for their fabrication. Numerous plant species have been utilized as precursors for the synthesis of NiO nanoparticles due to their various phytochemical compositions. Nevertheless, there are several key aspects that warrant further investigation in future studies.
- The precise mechanism underlying the involvement of plant extracts in the synthesis of NiO nanoparticles remains incompletely understood, necessitating more in-depth research. Exploring how different plant components, such as flower color, influence the synthesis process could provide valuable insights into optimizing the nanoparticle properties. Additionally, the impact of varying parameters like temperature and reaction duration on the morphological characteristics of NiO nanoparticles requires thorough examination to enhance the synthesis process efficiency and tailor the nanoparticles for specific applications.
- developed into these aspects and more than efficient, researchers can pave the way for more sustainable and controlled synthesis approaches that leverage the unique properties of plant extracts for NiO nanoparticle production.
- preparation methods to ensure a wide range of commercial uses. Based on theoretical predictions and experimental data, the designed and synthesized earth-abundant noble metal-free materials are based on nitrogen, phosphorus, molybdenum, sulfur, iron, nickel, manganese, carbon, etc.
- high efficiency.
- good durability over a period of at least several cycles.
- high chemical/catalytic stability over a wide pH (even at all pH values) and temperature ranges.
- low cost to ensure inexpensive hydrogen production.
- scalability of the catalysts.

Conclusion

Hydrogen from renewable energy can be produced everywhere, while the cost-effectiveness varies by location. Hydrogen enables renewable energy to be traded across borders in the form of molecules or commodities. The state of the art from the literature on hydrogen production under different technology routes is an important concern for researchers around the world looking at the cost and technical production potential of green hydrogen in different scenarios and assumptions. This research field provides a perspective on the role of hydrogen in climate change since H2 will be needed to again full decarbonization. In this sense, green hydrogen, produced from renewables, is expected to represent the main part of the production. Moreover, hydrogen allows the storage of renewable energy, which can be used to fuel transportation, generate heat for industrial processes, and send electricity to the grid. In this study, we focused on solar energy and wind energy, which are used as green sources to produce the electricity for powering electrolysis for hydrogen production. The applications of PV systems are more useful in remote areas to produce electricity where no grid is available. Moreover, producing hydrogen-based solar and wind energy to provide electricity for electrolysis units is very interesting, particularly in case of excess energy when the hydrogen can be sold or store or converted to electricity via fuel cell. The renewable hydrogen which has been 100% converted into electricity can be returned to the grid, effectively supplying solar or wind power when the sun is not shining and the wind is not blowing.

- ✓ Hydrogen is an alternate energy carrier that can be storedand transferred and has a high calorific value, making itsuited to replace fossil fuels
- ✓ Green production attracts more attention due to its ability to produce hydrogen with zero carbon emissions. How- ever, coupling the energy source with a water electrolyzer is a better production technique
- ✓ The electrolyzers can be divided into low-temperature electrolyzers (PEM, AWE, and AEM) and high-temper- ature electrolyzer (SOE). The low-temperature electrolyzers do not need any heat source and only require an electric source. However, a heat source helps to convert water to steam in SOE, including a power source forwater decomposition.
- ✓ The primary goal of commercializing a green hydro- gen production system is to reduce the capital invest- ment of its components and improve the components' efficiency. These enhancements will enable green hydrogen to compete with other production method the global market.

Nomenclature

A- Area (m2)

E- Equilibrium voltage (V)

ED- Exergy Destruction (kW)

G- Solar irradiance (W/m2)

I- Electric current (A)

j- Current density (A/m2)

P- Power (kW)/Pressure (bar)

q- Thermal power (kW)

T- Temperature (◦C)

U- Voltage (V)

B_g- permeability, m^2 Pa^{-1} s^{-1}

Cp,m- molar heat capacities of reactant/products m, J mol1 K1

D^{eff}_{H2O} - effective diffusion coefficient of H2O, m^2/s

E - equilibrium potential, V

E_T- total energy from solar concentrating beam splitting device, W

F- Faraday constant, C mol1

G- Gibbs free energy, J mol1

H- enthalpy, J mol1

HHV- higher heating value of H2, J mol1

I- electric current through the SOSE, A

I_L- electric current through the leakage resistance RL, A

I_T- total input electric current through the SOSE, A

j- current density, A m2

j_0- exchange current density, A m2

j_T- total input electric current density, A m2

j_T- total input electric current density corresponding tohmax,Am2

L_V- latent heat of water under 101.325 kPa, J mol1

n_e- number of electrons

P- input electric power, W

Q_J- Joule heat generated per unit time, W

Q_{SOSE} - thermal energy required for the SOSE per unit time,W

Q_{H2O}- thermal energy required for heating water per unittime, W

R- universal gas constant, J mol1 K1

R_I- equivalent internal resistance, U

R_L- equivalent leakage resistance, U

S- entropy, J mol1

V- potential, V

Greek letters

μ- dynamic viscosity, μP

€- efficiency of heat exchangers, dimensionless

η - efficiency, dimensionless

η_{comp} - efficiency of compressor, dimensionless

η_{max} - maximum value of efficiency, dimensionless

Subscript

a -anode

act- activation

c- cathode

con- concentration

e- electrolyte

max -maximum

T- total

REFERENCES

1. Use of plant based analytes for the synthesis of NiO nanoparticles in catalyzing electrochemical H2O2 production Raj Kumar Das, Animes Kumar Golder PII: S1572-6657(18)30383-7 DOI: doi:10.1016/j.jelechem.2018.05.029.
2. J. Li, Z. Ai, L. Zhang, Design of a neutral electro-Fenton system with Fe@Fe2O3/ACF composite cathode for wastewater treatment, J. Hazard. Mater. 164 (2009) 18–25.
3. R.K. Das, A.K. Golder, Impact of supporting electrolytes on the stability of TiO2-Ti counter electrode during H2O2 electrogeneration, Surf. Eng. Appl. Electrochem. 53 (2017) 570–579.
4. Z. Qiang, J.-H. Chang, C.-P. Huang, Electrochemical regeneration of Fe2+ in Fenton oxidation processes, Water Res. 37 (2003) 1308-1319.
5. K. Esquivel, L.G. Arriaga, F.J. Rodriguez, L. Martinez, L.A. Godinez, Development of a TiO2 modified optical fiber electrode and its incorporation into a photoelectrochemical reactor for wastewater treatment, Water Res. 43 (2009) 3593-3603.
6. Z. Qiang, J.-H. Chang, C.-P. Huang, Electrochemical generation of hydrogen peroxide from dissolved oxygen in acidic solution, Water Res. 36 (2002) 85-94.
7. C. Samanta, Direct synthesis of hydrogen peroxide from hydrogen and oxygen: An overview of recent developments in the process, Appl. Catal. A 350 (2008) 133–149.
8. H. Zhong, J. Wang, Q. Zhang, F. Meng, D. Bao, T. Liu, X. Yang, Z. Chang, J. Yan, X. Zhang, In situ coupling FeM (M = Ni, Co) with nitrogen-doped porous carbon toward highly efficient trifunctional electrocatalyst for overall water splitting and rechargeable Zn–air battery, Adv. Sustainable. Syst. 1 (2017) 1700020.
9. H. Zhong, J. Wang, Y. Zhang, W. Xu, W. Xing, D. Xu, Y. Zhang, X. Zhang, ZIF-8 derived graphene-based Nitrogen-Doped porous carbon sheets as highly efficient and durable oxygen reduction electrocatalysts, Angew. Chem. Int. Ed. 53 (2014) 14235-14239.
10. F. Meng, H. Zhong, D. Bao, J. Yan, X. Zhang, In situ coupling of strung Co4N and intertwined N−C fibers toward free-standing bifunctional cathode for robust, efficient, and flexible Zn−air batteries, J. Am. Chem. Soc. 138 (2016) 10226-10231.
11. F. Meng, H. Zhong, J. Yan, X. Zhang, Iron-chelated hydrogel-derived bifunctional oxygen electrocatalyst for high-performance rechargeable Zn–air batteries, Nano Res. 10 (2017) 4436-4447.
12. A.D. Pozzo, L.D. Palma, C. Merli, E. Petrucci, An experimental comparison of a graphite electrode and a gas diffusion electrode for the cathodic production of hydrogen peroxide, J. Appl. Electrochem. 35 (2005) 413-419
13. W.R.P. Barros, Q. Wei, G. Zhang, Shuhui Sun, M.R.V. Lanza, C. Tavares, Oxygen reduction to hydrogen peroxide on Fe3O4 nanoparticles supported on Printex carbon and Graphene, Electrochim. Acta 162 (2015) 263-270.
14. Y. Lin, J. Yu, Z. Xing, X. Guo, X. Yu, B. Tang, J. Zou, Enhanced generation of H2O2 and radicals on Co9S8/partly-graphitized carbon cathode for degradation of bio-refractory organic wastewater, Electrochim. Acta 213 (2016) 341-350.
15. W. Chen, S. Cai, Q.-Q. Ren, W. Wen, Y.-D. Zhao, Recent advances in electrochemical sensing for hydrogen peroxide: a review, Analyst 137 (2012) 49-58.

16. . J.F. Carneiro, M.J. Paulo, M. Siaj, A.C. Tavares, M.R.V. Lanza, Nb2O5 nanoparticles supported on reduced graphene oxide sheets as electrocatalyst for the H2O2 electrogeneration, J. Catal. 332 (2015) 51-61.
17. M.H.M.T. Assumpcao, A. Moraes, R.F.B. De Souza, M.L. Calegaro, M.R.V. Lanza , E.R. Leite, M.A.L. Cordeiro, P. Hammer, M.C. Santos, Influence of the preparation method and the support on H2O2 electro-generation using cerium oxide nanoparticles, Electrochim. Acta 111 (2013) 339-343.
18. A.G. Al-Sehemi, A.S. Al-Shihri, A. Kalam, G. Du, T. Ahmad, Microwave synthesis, optical properties and surface area studies of NiO nanoparticles, J. Mol. Struct. 1058 (2014) 56–61.
19. S. Farhadi, Z. Roostaei-Zaniyani, Simple and low-temperature synthesis of NiO nanoparticles through solid-state thermal decomposition of the hexa(ammine)Ni(II) nitrate, [Ni(NH3)6](NO3)2, complex, Polyhedron 30 (2011) 1244-1249.
20. M. Jin, G. Zhang, F. Yu, W. Li, W. Lu, H. Huang, Sponge-like Ni(OH)2–NiF2 composite film with excellent electrochemical performance, Phys. Chem. Chem. Phys. 15 (2013) 1601-1605.
21. M. Chen, L. Wang, H. Yang, S. Zhao, H. Xu, G. Wu, Nanocarbon/composite catalsyts for bifunctional oxygen reduction and evolution in reversible alkaline fuel cells: A mini review, J. Power Sources 375 (2017) 277-290.
22. M. El-Kemary, N. Nagy, I. El-Mehasseb, Nickel oxide nanoparticles: Synthesis and spectral studies of interactions with glucose, Mater. Sci. Semicond. Process. 16 (2013) 1747-1752.
23. M. Liu, J. Chang, J. Sun, L. Gao, Synthesis of porous NiO using NaBH4 dissolved in ethylene glycol as precipitant for high-performance supercapacitor, Electrochim. Acta 107 (2013) 9-15.
24. W.J. Duan, S.H. Lu, Z.L. Wu,Y.S. Wang, Size effects on properties of NiO nanoparticles grown in alkalisalts, J. Phys. Chem. C 116 (2012) 26043-26051.
25. L. Wang, G. Zhang, Y. Liu, W. Li, W. Lu, H. Huang, Facile synthesis of a mechanically robust and highly porous NiO film with excellent electrocatalytic activity towards methanol oxidation, Nanoscale 8 (2016) 11256-11263.
26. G. Zhang, L. Wang, Y. Liu, W. Li, F. Yu, W. Lu, H. Huang, Cracks bring robustness: a pre-cracked NiO nanosponge electrode with greatly enhanced cycle stability and rate performance, J. Mater. Chem. A 4 (2016) 8211-8218.
27. G. Zhang, W. Li, K. Xie, F. Yu, H. Huang, A one-step and binder-free method to fabricate hierarchical nickel-based supercapacitor electrodes with excellent performance, Adv. Funct. Mater., 2013, 23, 3675-3681.
28. O.I. Medvedeva, S.S. Kambulova, O.V. Bondar, A.R. Gataulina, N.A. Ulakhovich, A.V. Gerasimov, V.G. Evtugyn, I.F. Gilmutdinov, M.P. Kutyreva, Magnetic cobalt and cobalt oxide nanoparticles in hyperbranched polyester polyol matrix, J. Nanotechnol. 2017 (2017) 1-9.
29. J. Ryu, S.-W. Kim, K. Kang, C. Beum Park, Synthesis of diphenylalanine/cobalt oxide hybrid nanowires and their application to energy storage, ACS Nano 2010 (1) 159-164.
30. R.K. Das, A.K. Golder, Co3O4 spinel nanoparticles decorated graphite electrode: Biomediated synthesis and electrochemical H2O2 sensing, Electrochim. Acta 251 (2017) 415-426.

31. C. Kapoor, A. Kumar, A. Pattanayak, R. Gopi, H. Kalita, R.K. Avasthe, S. Bihani, Genetic diversity in local chow-chow (Sechium edule Sw.) germplasm of Sikkim, Indian J. Hill Fmg. 27 (2014) 130-134.
32. J. Cadena-Iniguez, L. Arevalo-Galarza, C.H. Avendano-Arrazate, M. Soto-Hernandez, L.M. Ruiz-Posadas, E. Santiago-Osorio, M. Acosta-Ramos, V.M. Cisneros-Solano, J.F. Aguirre-Medina, D. Ochoa-Martinez, Production, genetics, postharvest management and pharmacological characteristics of Sechium edule (Jacq.) Sw., Fresh Produce 1 (2007) 41-53.
33. J.K. Sharma, P. Srivastava, G. Singh, M.S. Akhtar, S. Ameen, Green synthesis of Co3O4 nanoparticles and their applications in thermal decomposition of ammonium perchlorate and dye-sensitized solar cells, Mater. Sci. Eng. B 193 (2015) 181-188.
34. Ch.V. Rao, A.K. Golder, pH dependent size control, formation mechanism and antimicrobial functionality of bio-inspired AgNPs, RSC Adv. 6 (2016) 95483-95493.
35. C. N. Chinnasamy, B. Jeyadevan, K. Shinoda, K. Tohji, Synthesis and magnetic properties of face-centered-cubic and hexagonal-close-packed Ni nanoparticles through polyol process, J. Appl. Phys. 97 (2005) 10J309.
36. . Xia, M. Yu, J. Hu, J. Feng, J. Chen, M. Shi, X. Weng, A model of interface-related enhancement based on the contrast between Co3O4 sphere and cube for electrochemical detection of hydrogen peroxide, Electrochem. Commun. 40 (2014) 67-70.
37. Ch.V. Rao, S.S. Bag, A.K. Golder, A biosynthesis route to nearly spherical AgNPs using chayote fruit extract, Environ. Prog. Sustain. Energy 36 (2017) 192-199.
38. H.-Q. Wang, X.-P. Fan, X.-H. Zhang, Y.-G. Huang, Q. Wu, Q.-C. Pan, Q.-Y. Li, In situ growth of NiO nanoparticles on carbon paper as a cathode for rechargeable Li-O2 batteries, RSC Adv.7 (2017) 23328-23333.
39.]. A.K. Barve, S.M. Gadegone, M.R. Lanjewar, R.B. Lanjewar, Synthesis and characterization of nickel oxide based nanocomposite material, International Journal of Engineering Research and Applications (IJERA) ISSN: 2248-9622, 2014.
40. F. Motahari, M.R. Mozdianfarda, M. Salavati-Niasari, Synthesis and adsorption studies of NiO nanoparticles in the presence of H2acacen ligand, for removing Rhodamine B in wastewater treatment, Process Saf. Environ. Prot. 93 (2015) 282-292.
41. M. Alagiri, S. Ponnusamy, C. Muthamizhchelvan, Synthesis and characterization of NiO nanopartilces by sol-gel method, J. Mater. Sci.: Mater. Electron. 23 (2012) 728-732.
42. R. Barnard, G.T. Crickmore, J.A. Lee, F.L. Tye, The cause of residual capacity in nickel oxyhydroxide electrodes, J. Appl. Electrochem. 10 (1980) 61-70.
43. N. Benetis, K. Holmen, J. Kowalewski, L. Nordenskiold, O. Wahlberg, Investigation of nickel(II)-ascorbic acid complex formation in aqueous solution using potentiometric measurements, optical spectroscopy and 13C NMR spectroscopy, Acta Chem. Scand. A 35 (1981) 513-520.
44. G.-Y. Huang, S.-M. Xu, G. Xu, L.-Y. Li, L.-F. Zhang, Preparation of fine nickel powders via reduction of nickel hydrazine complex precursors, Trans. Nonferrous Met. Soc. China 19 (2009) 389-393.

45. H.G. Cha, J.H. Sohn, Y. Park, K.J. Lee, M.H. Jung, J.-W. Lee, W. Shin, M.J. Kang, D. Y. Kim, Y.S. Kang, Hierarchical NiO hollow microspheres: electrochemical and magnetic properties, RSC Adv. 2 (2012) 9786-9790.
46. T. Carballo, M.V. Gil, X. Gomez, F. Gonzalez-Andres, A. Moran, Characterization of different compost extracts using Fourier-transform infrared spectroscopy (FTIR) and thermal analysis, Biodegrad. 19 (2008) 815-830.
47. N. Mironova-Ulmane, A. Kuzmin, I. Steins, J. Grabis, I. Sildos, M. Pars, Raman scattering in nanosized nickel oxide NiO, J. Phys. Conf. Series 93 (2007) 012039.
48. A. Rahdar, M. Aliahmad, Y. Azizi, NiO Nanoparticles: Synthesis and Characterization, JNS 5 (2015) 145-151.
49. L. Ai, Y. Zeng, Hierarchical porous NiO architectures as highly recyclable adsorbents for effective removal of organic dye from aqueous solution, Chem. Eng. J. 215-216 (2013) 269-278.
50. Photocatalytic activity of the biogenic mediated green synthesized CuO nanoparticles confned into MgAl LDH matrix HildanaTesfaye Berede1 , Dinsefa MensurAndoshe1 (2024) 14:2314 | https://doi.org/10.1038/s41598-024-52547-w.
51. Hydrogen Generation by Water Electrolysis Youssef Naimi and Amal Antar Additional information is available at the end of the chapter http://dx.doi.org/10.5772/intechopen.76814.
52. Janjua MBI, Leroy RL. Electrocatalyst performance in industrial water electrolysers. Inter- national Journal of Hydrogen Energy. 1985;10:11-19.
53. Stojić DL, Marčeta MP, Sovilj SP, Miljanić SS. Hydrogen generation from water electroly- sis—possibilities of energy saving. Journal of Power Sources. 2003;118:315.
54. Abdelshafy AM, Hassan H, Jurasz J (2018) Optimal design of a gridconnected desalination plant powered by renewable energy resources using a hybrid PSO–GWO approach. Energy Convers Manag 173:331–347. https://doi.org/10.1016/J.ENCONMAN. 2018.07.083
55. Abohamzeh E, Salehi F, Sheikholeslami M et al (2021) Review of hydrogen safety during storage, transmission, and applications processes. J Loss Prev Process Ind 72:104569. https://doi.org/10. 1016/j.jlp.2021.104569
56. Agaton CB, Batac KIT, Reyes EM (2022) Prospects and challenges for green hydrogen production and utilization in the Philippines. Int J Hydrog Energy 47:17859–17870. https://doi.org/10.1016/J. IJHYDENE.2022.04.101
57. Hassan IA, Ramadan HS, Saleh MA, Hissel D (2021) Hydrogen storage technologies for stationary and mobile applications: review, analysis and perspectives. Renew Sust Energ Rev 149:111311. https://doi.org/10.1016/J.RSER.2021.111311.
58. Hassan AA, Elwardany AE, Ookawara S, Hassan H (2022) Energy, exergy, economic and environmental (4E) assessment of hybrid solar system powering adsorption-parallel/series ORC multigeneration system. Process Saf Environ Prot 164:761–780. https:// doi.org/10.1016/J.PSEP.2022.06.024.
59. Hacker V, Fankhauser R, Faleschini G et al (2000) Hydrogen production by steam–iron process. J Power Sources 86:531–535. https:// doi.org/10.1016/S0378-7753(99)00458-9
60. Gupta RB (2009) Hydrogen Fuel. CRC Press, Boca Raton Gutiérrez-Martín F, Amodio L, Pagano M (2020) Hydrogen production by water electrolysis and of-grid solar PV. Int J Hydrog Energy. https://doi.org/10.1016/j.ijhydene.2020.09.098

61. Kovács KL, Maróti G, Rákhely G (2006) A novel approach for biohydrogen production. Int J Hydrog Energy 31:1460–1468. https:// doi.org/10.1016/j.ijhydene.2006.06.011
62. Nasser M, Megahed TF, Ookawara S, Hassan H (2022a) Performance evaluation of PV panels/wind turbines hybrid system for green hydrogen generation and storage: energy, exergy, economic, and enviroeconomic. Energy Convers Manag 267:115870. https:// doi.org/10.1016/j.enconman.2022.115870
63. Steinfeld A (2005) Solar thermochemical production of hydrogen - a review. Sol Energy 78:603–615. https://doi.org/10.1016/j.solen er.2003.12.012
64. Zhang F, Zhao P, Niu M, Maddy J (2016) The survey of key technologies in hydrogen energy storage. Int J Hydrog Energy 41:14535– 14552. https://doi.org/10.1016/j.ijhydene.2016.05.293
65. Holladay JD, Hu J, King DL, Wang Y (2009) An overview of hydrogen production technologies. Catal Today 139:244–260. https://doi. org/10.1016/j.cattod.2008.08.039
66. El-Emam RS, Özcan H (2019) Comprehensive review on the technoeconomics of sustainable large-scale clean hydrogen production. J Clean Prod 220:593–609. https://doi.org/10.1016/j.jclep ro.2019.01.309
67. David M, Ocampo-Martínez C, Sánchez-Peña R (2019) Advances in alkaline water electrolyzers: a review. J Energy Storage 23:392– 403. https://doi.org/10.1016/j.est.2019.03.001
68. Burton NA, Padilla RV, Rose A, Habibullah H (2021) Increasing the efciency of hydrogen production from solar powered water electrolysis. Renew Sust Energ Rev 135:110255. https://doi.org/10. 1016/j.rser.2020.110255
69. Buttler A, Spliethof H (2018) Current status of water electrolysis for energy storage, grid balancing and sector coupling via power to-gas and power-to-liquids: a review. Renew Sust Energ Rev 82:2440–2454
70. Mohamed Nasser1,2 · Tamer F. Megahed3,4 · Shinichi Ookawara5 · Hamdy Hassan1,6 https://doi.org/10.1007/s11356-022-23323-y.
71. Muhammad Younas, Sumeer Shafique, Ainy Hafeez, Fahad Javed, Fahad Rehman https://doi.org/10.1016/j.fuel.2022.123317.
72. Synthesis of NiO nanoparticles via green route using Ageratum conyzoides L. leaf extract and their catalytic activity Miessya Wardani1 , Yoki Yulizar1,* , Iman Abdullah1 , Dewangga Oky Bagus Apriandanu1 10.1088/1757-899X/509/1/012077.
73. Green synthesis of gallic acid-coated silver nanoparticles with high antimicrobial activity and low cytotoxicity to normal cells Dan Li a, Zuojia Liua, Ye Yuana, Yawen Liub,**, Fenglan Niua,* 2015
74. Green synthesis of iron oxide nanoparticles using Terminalia bellirica and Moringa oleifera fruit and leaf extracts: Antioxidant, antibacterial and thermoacoustic properties Gautham B. Jegadeesan * , K. Srimathi, N. Santosh Srinivas, S. Manishkanna, D. Vignesh.
75. Manjari, G., Saran, S., Arun, T., Rao, A. V. B. & Devipriya, S. P. Catalytic and recyclability properties of phytogenic copper oxide nanoparticles derived from Aglaia elaeagnoidea fower extract. J. Saudi Chem. Soc. 21, 610–618 (2017).
76. Zelekew, O. A. & Kuo, D.-H. Synthesis of a hierarchical structured NiO/NiS composite catalyst for reduction of 4-nitrophenol and organic dyes. RSC Adv. 7, 4353–4362 (2017).
77. Muthuvel, A., Jothibas, M. & Manoharan, C. Synthesis of copper oxide nanoparticles by chemical and biogenic methods: Photocatalytic degradation and in vitro antioxidant activity. Nanotechnol. Environ. Eng. 5, 1–19 (2020).

78. Gu, H., Chen, X., Chen, F., Zhou, X. & Parsaee, Z. Ultrasound-assisted biosynthesis of CuO-NPs using brown alga Cystoseira trinodis: Characterization, photocatalytic AOP, DPPH scavenging and antibacterial investigations. Ultrason. Sonochem. 41, 109–119 (2018).
79. Senobari, S. & Nezamzadeh-Ejhieh, A. A comprehensive study on the enhanced photocatalytic activity of CuO–NiO nanoparticles: Designing the experiments. J. Mol. Liq. 261, 208–217 (2018).
80. Hadia, N.M.A.; Shaban, M.; Ahmed, A.M.; Mohamed, W.S.; Alzaid, M.; Ezzeldien, M.; Hasaneen, M.F.; El Malti, W.; Abdelazeez, A.A.A.; Rabia, M. Photoelectrochemical Conversion of Sewage Water into H2 Fuel over the CuFeO2/CuO/Cu Composite Electrode. Catalysts 2023, 13, 456. https://doi.org/10.3390/ catal13030456
81. Electrochemical production of hydrogen in molten salt Kaiyu Xie , Ali Reza Kamali * https://doi.org/10.1016/j.enconman.2021.114980
82. Betül Gürünlü , Çiğdem Taşdelen Yücedağ, and Mahmut Rahim Bayramoğlu https://doi.org/10.1155/2020/7029601
83. Yinlong Zhu, *a Qian Lin,a Yijun Zhong,b Hassan A. Tahini, c Zongping Shao bd and Huanting Wang *a 10.1039/d0ee02485f
84. Sung-Woo Park,‡a Eun-Tae Yun,‡a Hyun Jung Shin,a Wooyul Kim, b Jaesang Leea and Dong-Wan Kim * 10.1039/d1ta01741a
85. Mohamed Rabia1,2 | N. M. A. Hadia3,4 | Osama M. Farid5 | Ahmed Adel A. Abdelazeez6 | S. H. Mohamed7,8 | Mohamed Shaban1, 10.1002/er.7963
86. Sameerah I. Al-Saeedi https://doi.org/10.3390/ mi14051047
87. Molecules | Free Full-Text | TiO2 as a Photocatalyst for Water Splitting—An Experimental and Theoretical Review (mdpi.com)
88. https://dx.doi.org/10.1016/j.apcatb.2023.123233
89. Abdelshafy AM, Hassan H, Jurasz J (2018) Optimal design of a gridconnected desalination plant powered by renewable energy resources using a hybrid PSO–GWO approach. Energy Convers Manag 173:331–347. https://doi.org/10.1016/J.ENCONMAN.2018.07.083
90. Abohamzeh E, Salehi F, Sheikholeslami M et al (2021) Review of hydrogen safety during storage, transmission, and applications processes. J Loss Prev Process Ind 72:104569. https://doi.org/10.1016/j.jlp.2021.104569
91. Agaton CB, Batac KIT, Reyes EM (2022) Prospects and challenges for green hydrogen production and utilization in the Philippines. Int J Hydrog Energy 47:17859–17870. https://doi.org/10.1016/J.IJHYDENE.2022.04.101
92. Akikur RK, Saidur R, Ping HW, Ullah KR (2014) Performance analysis of a co-generation system using solar energy and SOFC technology. Energy Convers Manag 79:415–430. https://doi.org/10.1016/j.enconman.2013.12.036
93. Akyuz E, Oktay Z, Dincer I (2012) Performance investigation of hydrogen production from a hybrid wind-PV system. Int J Hydrog Energy 37:16623–16630. https://doi.org/10.1016/j.ijhydene.2012.02.149
94. Al Zahrani AA, Dincer I (2016) Design and analysis of a solar tower based integrated system using high temperature electrolyzer for hydrogen production. Int J Hydrog Energy 41:8042–8056. https://doi.org/10.1016/j.ijhydene.2015.12.103
95. Allouhi A (2020) Management of photovoltaic excess electricity generation via the power to hydrogen concept: a year-round dynamic assessment using artifcial neural networks. Int J Hydrog Energy 45:21024–21039. https://doi.org/10.1016/j.ijhydene.2020.05.262

96. Almutairi K, Hosseini Dehshiri SS, Hosseini Dehshiri SJ et al (2021) A thorough investigation for development of hydrogen projects from wind energy: a case study. Int J Hydrog Energy 46:18795–18815.https://doi.org/10.1016/j.ijhydene.2021.03.061
97. Armijo J, Philibert C (2020) Flexible production of green hydrogen and ammonia from variable solar and wind energy: case study of Chile and Argentina. Int J Hydrog Energy 45:1541–1558. https://doi.org/10.1016/j.ijhydene.2019.11.028
98. Arregi A, Amutio M, Lopez G et al (2018) Evaluation of thermochemical routes for hydrogen production from biomass: a review. Energy Convers Manag 165:696–719. https://doi.org/10.1016/J.ENCONMAN.2018.03.089
99. Atiz A (2020) Comparison of three diferent solar collectors integrated with geothermal source for electricity and hydrogen production. Int J Hydrog Energy 45:31651–31666. https://doi.org/10.1016/j.ijhydene.2020.08.236
100. Atiz A, Karakilcik H, Erden M, Karakilcik M (2019) Assessment of electricity and hydrogen production performance of evacuated tube solar collectors. Int J Hydrog Energy 44:14137–14144. https://doi.org/10.1016/j.ijhydene.2018.09.100
101. Ayodele TRR, Mosetlhe TCC, Yusuf AAA, Ntombela M (2021) Optimal design of wind-powered hydrogen refuelling station for some selected cities of South Africa. Int J Hydrog Energy 46:24919–24930. https://doi.org/10.1016/j.ijhydene.2021.05.059.
102. Babatunde OM, Munda JL, Hamam Y (2022) Hybridized of-grid fuel cell/wind/solar PV /battery for energy generation in a small household: a multi-criteria perspective. Int J Hydrog Energy 47:6437–6452. https://doi.org/10.1016/J.IJHYDENE.2021.12.018
103. Balta MT, Kizilkan O, Yilmaz F (2016) Energy and exergy analyses of integrated hydrogen production system using high temperature steam electrolysis. Int J Hydrog Energy 41:8032–8041. https://doi.org/10.1016/j.ijhydene.2015.12.211
104. Bernal-Agustín JL, Dufo-López R (2010) Techno-economical optimization of the production of hydrogen from PV-wind systems connected to the electrical grid. Renew Energy 35:747–758. https://doi.org/10.1016/j.renene.2009.10.004
105. Bhandari R, Trudewind CA, Zapp P (2014) Life cycle assessment of hydrogen production via electrolysis - a review. J Clean Prod 85:151–163. https://doi.org/10.1016/j.jclepro.2013.07.048
106. Bhattacharyya R, Misra A, Sandeep KC (2017) Photovoltaic solar energy conversion for hydrogen production by alkaline water electrolysis: conceptual design and analysis. Energy Convers Manag 133:1–13. https://doi.org/10.1016/j.enconman.2016.11.057
107. Bicer Y, Dincer I (2017) Experimental investigation of a PV-coupled photoelectrochemical hydrogen production system. Int J Hydrog Energy 42:2512–2521. https://doi.org/10.1016/j.ijhydene.2016.02.098
108. Bilgen E (2001) Solar hydrogen from photovoltaic-electrolyzer systems. Energy Convers Manag 42:1047–1057. https://doi.org/10.1016/S0196-8904(00)00131-X
109. Burton NA, Padilla RV, Rose A, Habibullah H (2021) Increasing the efciency of hydrogen production from solar powered water electrolysis. Renew Sust Energ Rev 135:110255. https://doi.org/10.1016/j.rser.2020.110255
110. Buttler A, Spliethof H (2018) Current status of water electrolysis for energy storage, grid balancing and sector coupling via powerto-gas and power-to-liquids: a review. Renew Sust Energ Rev 82:2440–2454
111. Cai D, Bamisile O, Adebayo V et al (2020) Integration of wind turbine with heliostat based CSP/CPVT system for hydrogen production and polygeneration: a thermodynamic comparison. Int J Hydrog Energy. https://doi.org/10.1016/j.ijhydene.2020.11.106

112. Carmo M, Fritz DL, Mergel J, Stolten D (2013) A comprehensive review on PEM water electrolysis. Int J Hydrog Energy 38:4901–4934Carton JG, Olabi AG (2010) Wind/hydrogen hybrid systems: opportunity for Ireland's wind resource to provide consistent sustainable energy supply. Energy 35:4536–4544. https://doi.org/10.1016/j.energy.2010.09.010
113. Chadegani EA, Sharifshourabi M, Hajiarab F (2018) Comprehensive assessment of a multi-generation system integrated with a desalination system: modeling and analysing. Energy Convers Manag 174:20–32. https://doi.org/10.1016/j.enconman.2018.08.011
114. Chen X, Liu Q, Xu J et al (2020) Thermodynamic study of a hybrid PEMFC-solar energy multi-generation system combined with SOEC and dual Rankine cycle. Energy Convers Manag 226:113512. https://doi.org/10.1016/ j.enconman.2020.113512.
115. Chi J, Yu H (2018) Water electrolysis based on renewable energy for hydrogen production. Cuihua Xuebao/Chin J Catal 39:390–394 Chien FS, Ngo QT, Hsu CC et al (2021) Assessing the capacity of renewable power production for green energy system: a way forward towards zero carbon electrifcation. Environ Sci Pollut Res 28:65960–65973. https://doi.org/10.1007/S11356-021-15517-7/FIGURES/3
116. Cho MK, Park HY, Lee HJ et al (2018) Alkaline anion exchange membrane water electrolysis: efects of electrolyte feed method and electrode binder content. J Power Sources 382:22–29. https://doi.org/10.1016/j.jpowsour.2018.02.025
117. Herwartz S, Pagenkopf J, Streuling C (2021) Sector coupling potential of wind-based hydrogen production and fuel cell train operation in regional rail transport in Berlin and Brandenburg. Int J Hydrog Energy. https://doi.org/10.1016/j.ijhydene.2020.11.242
118. Holladay JD, Hu J, King DL, Wang Y (2009) An overview of hydrogen production technologies. Catal Today 139:244–260. https://doi.org/10.1016/j.cattod.2008.08.039
119. Hosseini SE, Butler B (2021) Design and analysis of a hybrid concentrated photovoltaic thermal system integrated with an organic
120. Rankine cycle for hydrogen production. J Therm Anal Calorim 144:763–778. https://doi.org/10.1007/s10973-020-09556-4
121. Hosseini SE, Wahid MA (2020) Hydrogen from solar energy, a clean energy carrier from a sustainable source of energy. Int J Energy Res 44:4110–4131. https://doi.org/10.1002/er.4930
122. Houaijia A, Roeb M, Monnerie N, Sattler C (2015) Solar power tower as heat and electricity source for a solid oxide electrolyzer: a case study. Int J Energy Res 39:1120–1130. https://doi.org/10.1002/er.3316
123. Huang Q, Shi Y, Wang Y et al (2015) Multi-turbine wind-solar hybrid system. Renew. Energy 76:401–407. https://doi.org/10.1016/j.renene.2014.11.060
124. Huang PH, Kuo JK, Wu ZD (2016) Applying small wind turbines and a photovoltaic system to facilitate electrolysis hydrogen production. Int J Hydrog Energy 41:8514–8524. https://doi.org/10.1016/j.ijhydene.2016.02.051
125. IEA (2020) Projected Costs of Generating Electricity 2020 – Analysis - IEA.https://www.iea.org/reports/projected-costs-of-generating-electricity-2020. Accessed 26 Jul 2022
126. Iqbal MT (2003) Simulation of a small wind fuel cell hybrid energy system. Renew Energy 28:511–522. https://doi.org/10.1016/S0960-1481(02)00070-8
127. Iqbal W, Yumei H, Abbas Q et al (2019) Assessment of wind energy potential for the production of renewable hydrogen in Sindh Province of Pakistan. Processes 7:196. https://doi.org/10.3390/pr7040196IRENA2022 Workbook: IRENA_Electrolysers_Patents_Insights.https://public.tableau.com/views/IRENA_Electrolysers_Patents_Insights/Electrolysers_patent_insight?:showVizHome=no&embed=yes. Accessed 29 Jul 2022

128. Ishaq H, Dincer I (2020) Evaluation of a wind energy based system for co-generation of hydrogen and methanol production. Int J Hydrog Energy 45:15869–15877. https://doi.org/10.1016/j.ijhydene.2020.01.037
129. Ishaq H, Siddiqui O, Chehade G, Dincer I (2021) A solar and wind driven energy system for hydrogen and urea production with CO2 capturing. Int J Hydrog Energy 46:4749–4760. https://doi.org/10.1016/j.ijhydene.2020.01.208
130. Ismail TM, Ramzy K, Elnaghi BE et al (2019) Using MATLAB to model and simulate a photovoltaic system to produce hydrogen. Energy Convers Manag 185:101–129. https://doi.org/10.1016/j.enconman.2019.01.108
131. Joshi AS, Dincer I, Reddy BV (2010) Exergetic assessment of solar hydrogen production methods. Int J Hydrog Energy 35:4901–4908. https://doi.org/10.1016/j.ijhydene.2009.09.067
132. Joshi AS, Dincer I, Reddy BV (2011) Solar hydrogen production: a comparative performance assessment. Int J Hydrog Energy 36:11246–11257. https://doi.org/10.1016/j.ijhydene.2010.11.122
133. Khalilnejad A, Riahy GH (2014) A hybrid wind-PV system performance investigation for the purpose of maximum hydrogen production and storage using advanced alkaline electrolyzer. Energy Convers Manag 80:398–406. https://doi.org/10.1016/j.enconman.2014.01.040
134. Khan AA, Khan SU, Ali MAS et al (2022) Identifying impact of international trade and renewable energy consumption on environmental quality improvement and their role in global warmingEnviron Sci Pollut Res 29:33935–33944. https://doi.org/10.1007/S11356-022-18574-8/TABLES/7
135. Khatiwada D, Vasudevan RA, Santos BH (2022) Decarbonization of natural gas systems in the EU – costs, barriers, and constraints of hydrogen production with a case study in Portugal. Renew Sust Energ Rev 168:112775. https://doi.org/10.1016/J.RSER.2022.112775
136. Khelfaoui N, Djafour A, Ghenai C et al (2020) Experimental investigation of solar hydrogen production PV/PEM electrolyser performance in the Algerian Sahara regions. Int J Hydrog Energy 46:30524–30538. https://doi.org/10.1016/j.ijhydene.2020.11.193
137. Khouya A (2020) Levelized costs of energy and hydrogen of wind farms and concentrated photovoltaic thermal systems. A case study in Morocco. Int J Hydrog Energy 45:31632–31650. https://doi.org/10.1016/j.ijhydene.2020.08.240
138. Khouya A (2021) Hydrogen production costs of a polymer electrolyte membrane electrolysis powered by a renewable hybrid system. Int J Hydrog Energy 46:14005–14023. https://doi.org/10.1016/j.ijhydene.2021.01.213
139. Koleva M, Guerra OJ, Eichman J et al (2021) Optimal design of solardriven electrolytic hydrogen production systems within electricity markets. J Power Sources 483:229183. https://doi.org/10.1016/j.jpowsour.2020.229183
140. Koumi Ngoh S, Ayina Ohandja LM, Kemajou A, Monkam L (2014) Design and simulation of hybrid solar high-temperature hydrogen production system using both solar photovoltaic and thermal energy. Sustain Energy Technol Assess 7:279–293. https://doi.org/10.1016/j.seta.2014.05.002
141. Kovács KL, Maróti G, Rákhely G (2006) A novel approach for biohydrogen production. Int J Hydrog Energy 31:1460–1468. https://doi.org/10.1016/j.ijhydene.2006.06.011
142. Lagorse J, Simões MG, Miraoui A, Costerg P (2008) Energy cost analysis of a solar-hydrogen hybrid energy system for stand-alone applications. Int J Hydrog Energy 33:2871–2879. https://doi.org/10.1016/j.ijhydene.2008.03.054
143. Lahoussine Ouali HA, Moussaoui MA, Mezrhab A (2020) Hydrogen production from two commercial dish/Stirling systems compared to the photovoltaic system-case study: Eastern

Morocco. Appl Sol Energy (English Transl Geliotekhnika) 56:466–476. https://doi.org/10.3103/S0003701X20060080
144. Li C, Baek J-BB (2021) The promise of hydrogen production from alkaline anion exchange membrane electrolyzers. Nano Energy 87:106162Li G, Li J, Yang R, Chen X (2022a) Performance analysis of a hybrid hydrogen production system in the integrations of PV/T power generation electrolytic water and photothermal cooperative reaction. Appl Energy 323:119625. https://doi.org/10.1016/J.APENERGY.2022.119625
145. Li H, Cao X, Liu Y et al (2022b) Safety of hydrogen storage and transportation: an overview on mechanisms, techniques, and challenges. Energy Rep 8:6258–6269. https://doi.org/10.1016/J.EGYR.2022.04.067
146. Lim T, Kim SK (2022) Non-precious hydrogen evolution reaction catalysts: stepping forward to practical polymer electrolyte membrane-based zero-gap water electrolyzers. Chem Eng J 433:133681. https://doi.org/10.1016/J.CEJ.2021.133681
147. Lin H, Wu Q, Chen X et al (2021) Economic and technological feasibility of using power-to-hydrogen technology under higher wind penetration in China. Renew Energy 173:569–580. https://doi.org/10.1016/j.renene.2021.04.015
148. Liu J, Abbas Q, Alharthi M et al (2021) Managerial policy and economic analysis of wind-generated renewable hydrogen for light-duty vehicles: green solution of energy crises. Environ Sci Pollut Res 28:10642–10653. https://doi.org/10.1007/S11356-020-11018-1/TABLES/9
149. Luo Z, Wang X, Wen H, Pei A (2022) Hydrogen production from ofshore wind power in South China. Int J Hydrog Energy. https://doi.org/10.1016/J.IJHYDENE.2022.03.162
150. Younas M, Shafque S, Hafeez A et al (2022) An overview of hydrogen production: current status, potential, and challenges. Fuel
151. 316:123317. https://doi.org/10.1016/J.FUEL.2022.123317
152. Zafar S, Dincer I (2014) Thermodynamic analysis of a combined PV/Tfuel cell system for power, heat, fresh water and hydrogen production. Int J Hydrog Energy 39:9962–9972. https://doi.org/10.
153. 1016/j.ijhydene.2014.04.127
154. Zayed ME, Zhao J, Elsheikh AH et al (2021) A comprehensive review on dish/Stirling concentrated solar power systems: design, optical and geometrical analyses, thermal performance assessment, and applications. J Clean Prod 283:124664. https://doi.org/10.1016/j.jclepro.2020.124664
155. Zhang Y, Wei W (2020) Model construction and energy management system of lithium battery, PV generator, hydrogen production unit and fuel cell in islanded AC microgrid. Int J Hydrog Energy 45:16381–16397. https://doi.org/10.1016/j.ijhydene.2020.04.155
156. Zhang XR, Yamaguchi H, Uneno D et al (2006) Analysis of a novel solar energy-powered Rankine cycle for combined power and heat generation using supercritical carbon dioxide. Renew Energy 31:1839–1854. https://doi.org/10.1016/j.renene.2005.09.024
157. Zhang F, Zhao P, Niu M, Maddy J (2016) The survey of key technologies in hydrogen energy storage. Int J Hydrog Energy 41:14535–14552. https://doi.org/10.1016/j.ijhydene.2016.05.293
158. Zhou T, Francois B (2009) Modeling and control design of hydrogen production process for an active hydrogen/wind hybrid power system. Int J Hydrog Energy 34:21–30. https://doi.org/10.1016/j.ijhydene.2008.10.030.